

AD-A125 792

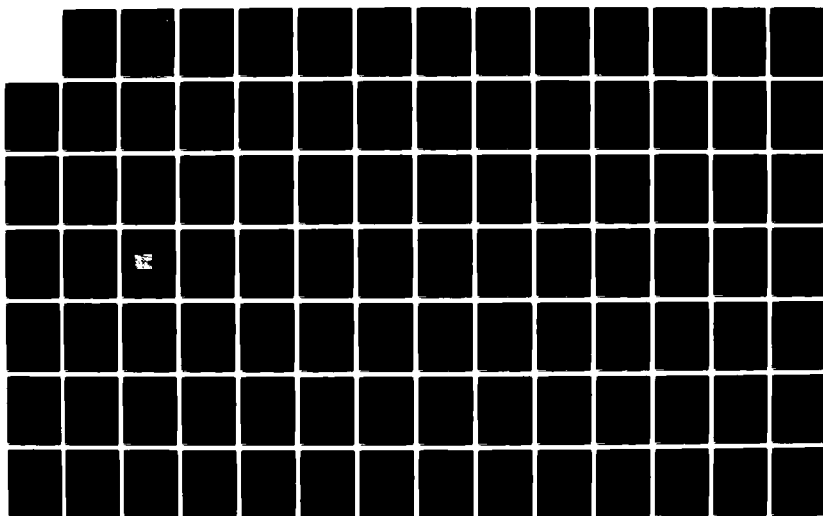
NUMERICAL WAKE PREDICTION METHODS FOR SUBMERGED
APPENDED BODIES A LITERAT..(U) DAVID W TAYLOR NAVAL
SHIP RESEARCH AND DEVELOPMENT CENTER BET.. C SUNG
FEB 83 DTNSRDC/SPD-1057-01

1/2

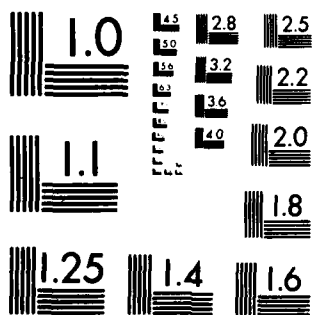
UNCLASSIFIED

F/G 20/4

NL



M-2



MICROCOPY RESOLUTION TEST CHART
NATIONAL BUREAU OF STANDARDS-1963-A

AD A 125792

DTIC FILE COPY

NUMERICAL WAKE PREDICTION METHODS FOR SUBMERGED APPENDED
BODIES, A LITERATURE SURVEY

by Chao-Ho Sung

DTNSRDC/SPD-1057-01

**DAVID W. TAYLOR NAVAL SHIP
RESEARCH AND DEVELOPMENT CENTER**

Bethesda, Maryland 20084



NUMERICAL WAKE PREDICTION METHODS FOR SUBMERGED
APPENDED BODIES, A LITERATURE SURVEY

by

Chao-Ho Sung

APPROVED FOR PUBLIC RELEASE: DISTRIBUTION UNLIMITED

SHIP PERFORMANCE DEPARTMENT
DEPARTMENTAL REPORT

MAR 17 1983

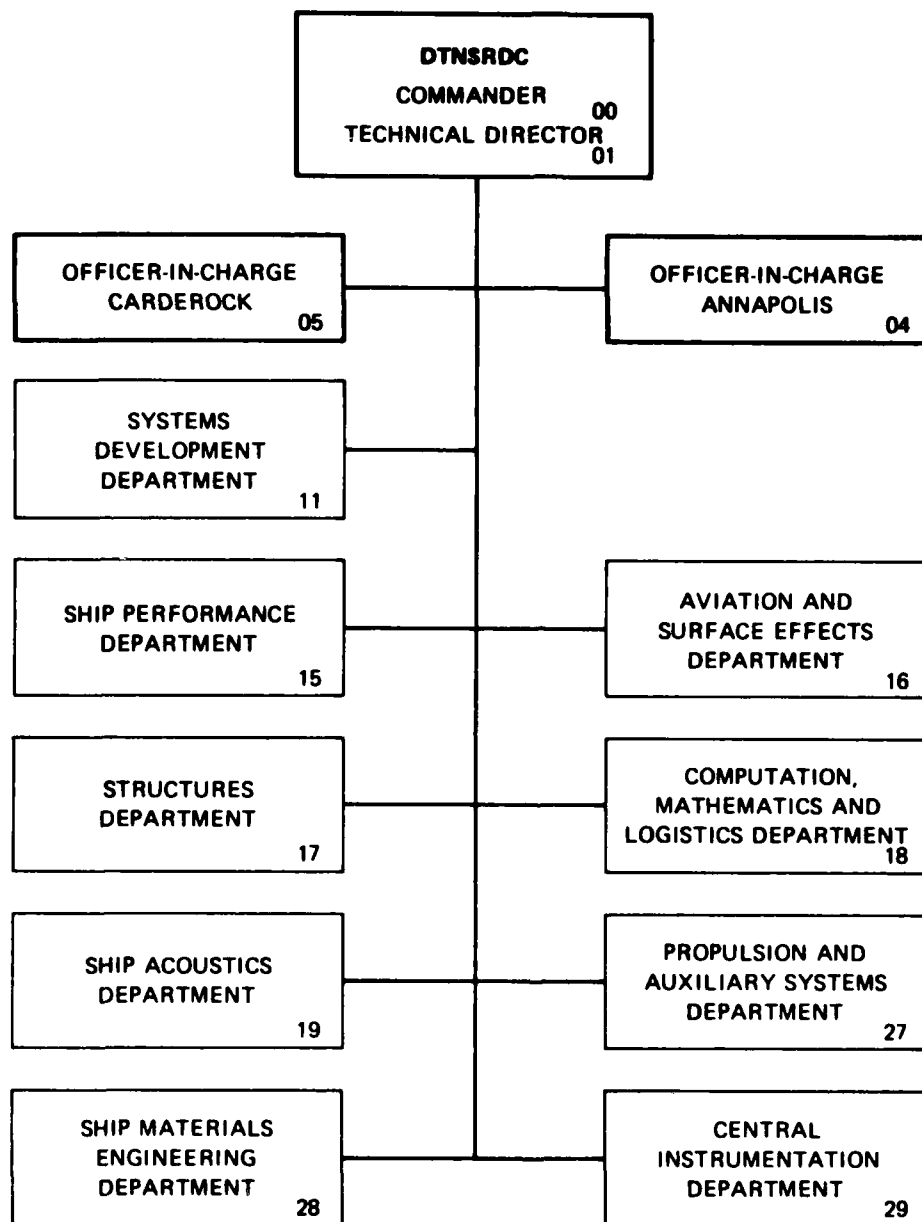
A

FEBRUARY 1983

DTNSRDC/SPD-1057-01

83 03 17 075

MAJOR DTNSRDC ORGANIZATIONAL COMPONENTS



UNCLASSIFIED

SECURITY CLASSIFICATION OF THIS PAGE (When Data Entered)

REPORT DOCUMENTATION PAGE		READ INSTRUCTIONS BEFORE COMPLETING FORM
1. REPORT NUMBER DTNSRDC/SPD-1057-01	2. GOVT ACCESSION NO. AD A125 792	3. RECIPIENT'S CATALOG NUMBER
4. TITLE (and Subtitle) NUMERICAL WAKE PREDICTION METHODS FOR SUBMERGED APPENDED BODIES, A LITERATURE SURVEY		5. TYPE OF REPORT & PERIOD COVERED Final
		6. PERFORMING ORG. REPORT NUMBER
7. AUTHOR(s) Chao-Ho Sung		8. CONTRACT OR GRANT NUMBER(s)
9. PERFORMING ORGANIZATION NAME AND ADDRESS David W. Taylor Naval Ship R&D Center Bethesda, Maryland 20084		10. PROGRAM ELEMENT, PROJECT, TASK AREA & WORK UNIT NUMBERS Program Element: 62543N Task Area: SF 43-421 Work Unit No. 1-1506-202-11
11. CONTROLLING OFFICE NAME AND ADDRESS Naval Sea Systems Command (05R) Washington, D.C. 20362		12. REPORT DATE February 1983
		13. NUMBER OF PAGES vi+95
14. MONITORING AGENCY NAME & ADDRESS (if different from Controlling Office)		15. SECURITY CLASS. (of this report) UNCLASSIFIED
		15a. DECLASSIFICATION/DOWNGRADING SCHEDULE
16. DISTRIBUTION STATEMENT (of this Report) APPROVED FOR PUBLIC RELEASE: DISTRIBUTION UNLIMITED		
17. DISTRIBUTION STATEMENT (of the abstract entered in Block 20, if different from Report)		
18. SUPPLEMENTARY NOTES		
19. KEY WORDS (Continue on reverse side if necessary and identify by block number) Submerged Appended Bodies Wake Prediction Turbulent Boundary Layers		
20. ABSTRACT (Continue on reverse side if necessary and identify by block number) The numerical methods relevant to the wake prediction of submerged appended bodies for the purpose of predicting full scale wake are surveyed. The main flow features are first described and the numerical techniques used to predict them are then discussed. A complete solution of the flows around submerged appended bodies is beyond the reach of the state-of-the-art, both numerically and computerwise. For this reason, two approaches are recommended to be pursued simultaneously. One approach is for immediate applications and the other approach for long-range research. For the first approach, the		

DD FORM 1 JAN 73 1473

EDITION OF 1 NOV 65 IS OBSOLETE
S/N 0102-LF-014-6601

UNCLASSIFIED

SECURITY CLASSIFICATION OF THIS PAGE (When Data Entered)

momentum integral method is recommended due to its relative simplicity and its flexibility to adapt to experimental data. For the second approach, a numerical procedure no less sophisticated than the one by solving the partially parabolic Navier-Stokes equations with the κ - ϵ turbulence model should be considered.



TABLE OF CONTENTS

	Page
LIST OF FIGURES	iv
LIST OF TABLES	v
LIST OF ABBREVIATIONS AND SYMBOLS	vi
ABSTRACT	1
ADMINISTRATIVE INFORMATION	1
INTRODUCTION	1
PHYSICS OF THE PROBLEM	3
UNAPPENDED BODIES OF REVOLUTION	3
APPENDED BODIES	5
NUMERICAL METHODS	9
FINITE DIFFERENTIAL METHODS	10
MOMENTUM INTEGRAL METHODS	13
POTENTIAL FLOW METHODS	15
COMPARISON OF NUMERICAL METHODS	17
NUMERICAL TREATMENT OF MAIN FLOW FEATURES RELEVANT TO APPENDED BODIES.....	18
THICK TURBULENT BOUNDARY LAYER	18
FLOW SEPARATION	21
SECONDARY FLOW	22
WAKE	24
SUMMARY AND RECOMMENDATIONS	25
APPENDIX A - ALPHABETICAL BIBLIOGRAPHY OF THE LITERATURE SURVEYED	42
(with tabularized highlights of the Bibliography on page 60)	
REFERENCES	86

LIST OF FIGURES

	Page
1 - Variation of Boundary-Layer Thickness and Local Radius of the Body	28
2 - Variation of Wall Static Pressure, Pressure and Velocity at the Edge of the Boundary Layer	28
3 - Mixing-Length Profiles	29
4 - Variation of the Axial Reynolds Shear Stress	29
5 - Flow Field of the Appendage/Body Junction	30
6 - Wake of the Appendage/Body Junction Induced Flow Field	30
7 - Non-Crossover Type of Crossflow	31
8 - Crossover Type (or S-Shaped) of Crossflow	31
9 - Streamline Patterns of Horseshoe Vortices (Laminar Flow).....	32
10 - Comparison Between Experimental Laminar and Turbulent Flows About 2:1 and 4:1 Ovals	33
11a - Idealized Wing/Body Junction	34
11b - Secondary Flow Vectors at a Downstream Station $X = 1223$ mm of the Idealized Wing/Body Junction	34
12 - Comparison of Experiment and Computation of the Separation Line in Front of the Cylinder/Flat-Plate Junction	35

LIST OF TABLES

	Page
1 - Levels of Approximation and the State-of-the-Art of Computational Fluid Dynamics	36
2 - Status and Outlook of Computational Fluid Dynamics	37
3 - Development of Computational Aerodynamics	38
4 - Classification of the Governing Equations	39
5 - Comparison of Numerical Methods	40
6 - Methods to Account for Thick Turbulent Boundary Layers	41
A1 - Highlights of the Bibliography	68

LIST OF ABBREVIATIONS AND SYMBOLS

$C_{p\delta}$	Static pressure coefficient at the edge of the boundary layer
C_{pw}	Static pressure coefficient at the wall
2-D, 3-D	Two-dimensional and three-dimensional respectively
ℓ	Mixing length
Q_δ	Resultant velocity at the edge of the boundary layer
r_o	Local radius of the body of revolution
U, U_e	Free stream velocity at the edge of the boundary layer
U_∞	Free stream velocity at infinity
U_{ref}	Reference velocity of the incoming free stream to the body of revolution
$\overline{u'v'}$	Axial Reynolds shear stress
u	Mean velocity in the free streamwise direction
w	Mean velocity in the crossflow direction
X/L	Ratio of the distance from the nose of the body of revolution to the
L	total length of the body of revolution
x, y, z	Cartesian coordinates
y	Normal distance to the wall
α_w	Angle between the direction of the free stream and the direction of the limiting wall streamline
δ	Thickness of the boundary layer
δ^*	Displacement thickness of the boundary layer
$\kappa - \epsilon$	κ is the kinetic energy of turbulence and ϵ its dissipation rate
τ_o	Wall shear stress
ξ, η, ζ	Orthogonal curvilinear coordinates

ABSTRACT

The numerical methods relevant to the wake prediction of submerged appended bodies for the purpose of predicting full scale wake are surveyed. The main flow features are first described and the numerical techniques used to predict them are then discussed. A complete solution of the flows around submerged appended bodies is beyond the reach of the state-of-the-art, both numerically and computerwise. For this reason, two approaches are recommended to be pursued simultaneously. One approach is for immediate applications and the other approach for long-range research. For the first approach, the momentum integral method is recommended due to its relative simplicity and its flexibility to adapt to experimental data. For the second approach, a numerical procedure no less sophisticated than the one by solving the partially parabolic Navier-Stokes equations with the $\kappa-\epsilon$ turbulence model should be considered.

Kappa Epsilon

ADMINISTRATIVE INFORMATION

This investigation was authorized and funded by the Office of Naval Technology Ships Submarines and Boats Exploratory Development Program, under the management of the Naval Sea Systems Command, Code 05R, Program Element 62543N, Task Area 421-252, Work Unit number 1-1506-202-11.

INTRODUCTION

In order to design a propeller for a submerged vehicle, it is essential to know the velocity field (i.e. wake) in the propeller plane. One of the goals of the application of computational fluid dynamics to ship design is to develop numerical techniques such that the wake in the propeller plane can be predicted. Once an analytical prediction method has been developed, model tests for the purpose of obtaining wake data will be either unnecessary or would be needed only at the final stage of design. Before such a goal can be achieved, full scale wake data must be obtained from model wake data by an appropriate extrapolation method in order to account for Reynolds number effect.

In the case of submerged appended bodies, numerical techniques have been developed for the prediction of the wake of bodies of revolution, but numerical techniques are not available to predict the wake behind appended bodies. Thus, currently the full scale wake of a submerged appended body is obtained by the superposition of the predicted full scale wake of the bare body and a correction due to the presence of the appendages. Since the correction is based on model test data, the Reynolds number effect due to the presence of the appendages has been completely neglected. The development of numerical wake prediction methods which recognize the presence of the appendages will undoubtedly improve the accuracy of the predicted full scale wake. The objective of this report is to survey available numerical techniques which are relevant to the wake prediction of submerged appended bodies and to recommend approaches which appear promising.

The wake predicted in the absence of the propulsor (i.e. nominal wake) is modified by the influence of an operating propeller. This report will not include a survey of the techniques used to account for wake/propulsor interactions; only numerical techniques which are relevant to the prediction of the nominal wakes of submerged appended bodies will be surveyed.

As it will become evident later, the flow around an appended body has not been solved successfully for the application described above. Therefore, it is not possible to give a critical review of the numerical techniques available to solve the problem. Instead, the numerical techniques which have been used in other research fields, such as aerodynamics and turbomachinery, to solve the flow problems relevant to the one considered here will be surveyed and introduced.

At present, limitation of both the numerical technique and computer capability make it unfeasible to attempt to compute the wake fields of appended bodies by solving the full Navier-Stokes equations. It is therefore necessary to simplify the governing equations and, consequently, it is also necessary to select a turbulence closure model appropriate to the problem considered. To do both, it is essential to understand the physics of the problem considered. Thus, the main flow characteristics of unappended bodies will be discussed first and then the major complications of the flow field due to the presence of the appendage will be described. The discussion of various numerical methods and turbulence closure models commonly used in turbulent boundary layer calculations will follow. Advantages and disadvantages of these methods and models will be mentioned based on comparisons of numerical methods that took place in several international conferences. This will be followed by a review of the specific numerical techniques used in the treatment of the main flow features relevant to appended bodies. Based on the above discussion, recommendation of promising approaches will be made.

In addition to the ninety two references given for the above discussion, an alphabetical bibliography of the literature surveyed, which includes the ninety two references mentioned, is also given in the Appendix. Highlights of the bibliography are given in Table A1 of the Appendix.

PHYSICS OF THE PROBLEM

UNAPPENDED BODIES OF REVOLUTION

Extensive measurements of mean velocity, pressure, Reynolds stress and skin friction have been made on various axisymmetric bodies of revolution with emphasis on stern and near wake regions. Of particular interest are the works of the two

research teams led by Patel^{1,2*} and Huang³. The main flow feature is that the thickness of the turbulent boundary layer is in the same order of magnitude as the local body radius in the stern region at locations greater than, say, 90 percent of the total body length ($X/L = 0.9$) for an axisymmetric body, as illustrated in Figure 1, taken from Reference 1. The main characteristics of a thick boundary layer may be summarized as:

1. A large increase of the pressure coefficient from the edge of the boundary layer to the wall as shown in Figure 2. The increase is about 70 percent at $X/L = 0.95$ and about 100 percent at $X/L = 0.99$.
2. The mixing length in the thick boundary layer is shortened by more than 50 percent compared to that in the upstream region of the thin boundary layer as shown in Figure 3.
3. Reynolds shear stresses are less intensive in the thick boundary layer region, but spread out more. The variation of the axial Reynolds shear stress is shown in Figure 4 to illustrate this point.

Analogous characteristics have also been observed in the near wake region².

From the point of view of seeking numerical solutions in the thick turbulent boundary layer, characteristic (1) implies that the governing equations based on the standard thin boundary layer approximation require modifications to account for the pressure variation across the boundary layer, and characteristics (2) and (3) imply that the turbulence closure models, in particular the eddy-viscosity model which is based on the mixing length concept, must also be modified accordingly.

There are several mechanisms which cause the thick boundary layer. Among them are the adverse pressure gradient in the streamwise direction, the divergence of mean-flow streamlines in planes normal to the body surface and the transverse

*References are listed on page 86.

surface curvature effect. The first two effects are the results of a relatively large streamwise surface curvature in the stern region of the body of revolution. The effect of the transverse* surface curvature on the pressure variation across the boundary layer is not large. For example, as the flow streams downward along the surface of a long slender cylinder of constant radius (i.e. large transverse curvature), the boundary layer thickness can become several times larger than the radius of the cylinder. However, the rate of increase of the displacement thickness is small and the pressure variation across the boundary layer is not large much like the thin boundary layer of a flat plate. The comparison of measurements and the computations by Cebeci⁴ confirms that for this type of flow, the thin boundary layer approximation is adequate. The above discussion leads to the conclusion that the main cause of the thick boundary layer where the pressure varies significantly across the boundary layer is the convex longitudinal surface curvature in the stern region where the streamlines converge. As the flow streams along the curved surface, a large pressure gradient is generated in order to balance the centrifugal force applied on fluid particles along a curved streamline.

APPENDED BODIES

Most of the theoretical and experimental investigations of flows around appended bodies were carried out in relation to the wing/fuselage junction flows in aircrafts and the blade/end-wall flows in turbomachines. These two areas of research are the main sources of this survey in the attempt to understand the physical phenomena involved in flows around appended bodies and to search for promising numerical approaches to predict them.

The complexity of the flow field around an appended body is shown schematically in Figure 5 taken from Reference 5. The resulting wake shown in

*Transverse is used here to mean: transverse to the streamwise flow direction.

Figure 6 indicates the importance of the interference effect between the appendage and the body. A further indication of the importance of the interference effect between a body of revolution and a tail fin has been demonstrated in the wake measurements by Sevik⁶

The flow field of the appendage/body junction as shown in Figure 5 can be divided into three regions:

1. The longitudinal flow-reversal region: This is the region between the singular separation point and the leading edge of the appendage (strut stagnation line). The horseshoe vortex is generated in this region.
2. The transverse flow-reversal region: This region is the passage of the horseshoe vortex along the two sides of the appendage/body junction and is downstream of the longitudinal flow-reversal region.
3. The crossflow region: This is the region outside of the above two regions that are enclosed by the line of ordinary separation, or what is also called the primary separation line.

These flow features have been observed by flow visualization techniques^{5,7-10} and can be explained as follows.

Suppose the appendage (a wing or a cylinder) is mounted on a flat plate or on an axisymmetric body of revolution, then the boundary layer far upstream of the appendage is two-dimensional. The two-dimensionality of the flow will be destroyed by the pressure force generated by the presence of the appendage. This pressure force tends to push the fluid away from the appendage. Since the fluid particles near the wall of the body have been slowed down by the wall friction, the inertial force near the wall is smaller than the inertial force away from the wall and is more easily overcome by the pressure force. Thus, the interaction

between the inertial and the pressure forces causes the flow to reverse in the longitudinal direction in region (1) as shown in Figure 5, generating the horseshoe vortex. The vorticity line of the horseshoe vortex then bends around the appendage like a necklace, resulting in streamwise vortices in region (2) with their directions as shown in Figure 5. There are two types of crossflows in region (3), one is the non-crossover type as shown in Figure 7 and the other is the crossover type as shown in Figure 8. The non-crossover crossflow occurs in the upstream and the downstream position away from the inflection point of the S-shaped streamline as shown in Figure 5 while the crossover crossflow occurs in the neighborhood of the inflection point where the direction of the curvature of the free-stream streamline is reversed. The direction of the crossflow upstream of the inflection point is the same as that shown in Figure 7, but the direction is reversed downstream of the inflection point since the direction of the curvature of the freestream streamline is reversed resulting in the reversal of the direction of the centrifugal force. Both types of crossflows are pressure-driven. Consequently, rapid changes in the crossflow profile take place near the wall and little changes occur near the edge of the boundary layer where the pressure force is approximately balanced by the centrifugal force generated by the curvature of the streamline. For a further discussion of both types of crossflows, one is referred to the papers by Klinksieck and Pierce¹¹ and by Prahlad¹².

The laminar horseshoe vortex has been observed to form in systems of 2, 4, or 6 vortices as shown schematically in Figure 9 (taken from Reference 7). However, two vortices are predominant in the turbulent boundary layer and furthermore, these two vortices tend to merge into one as shown by Peake et al⁸ in Figure 10. This is further confirmed by the measurement of the velocity vector downstream

of the leading edge of the wing by Shabaka and Bradshaw¹³ shown in Figures 11a and 11b. The implication of this observation is that, if the detailed flow features in region (1) are not of major concern, the flow field can be assumed as being generated by a single horseshoe vortex. This assumption is important in modelling the streamwise vortex motion in region (2) when momentum integral methods are used.

The separation point at the leading edge of region (1) is a singular point with zero skin friction¹⁰. But the skin friction is not zero along the primary separation line¹⁰; rather it is a line along which the wall limiting streamlines from region (3) and those from regions (1) and (2) converge. Further discussion of the type and of the nature of flow separations can be found in References 14-17.

Another feature of turbulent boundary layers with flow separations or with large crossflows is that the direction of the velocity gradient vector differs significantly from that of the shear stress vector even near the wall. This anisotropic property of the shear stress has been observed by several investigators under different experimental conditions¹⁸⁻²⁰. The implication of this property is that the simple eddy-viscosity and the mixing-length models, which automatically lead to the coincidence of these two vectors, may not be adequate turbulence closure models for this type of problem.

The size of the horseshoe vortex region depends on the geometry of the appendage^{8,21}, and more importantly on the thickness of the incoming turbulent boundary layer near the location of the singular separation point^{5,21}. Thus, referring to a body of revolution (see Figure 1), if a tail fin is placed at 95 percent length of the body where the thickness of the boundary layer is approximately equal to the local radius of the body, then the size of the horseshoe vortex

region is approximately in the order of the local radius of the body. On the other hand, if a fin is placed close to the nose of the body then, the horseshoe vortex region generated will be rather small since the thickness of the boundary layer at that location is very thin.

NUMERICAL METHODS

Several papers have discussed the state-of-the-art and the outlook of computational fluid dynamics. In the 1980 symposium on the "Computation of Viscous - Inviscid Interaction", Le Balleur²² divided the numerical approximations used in the computation of laminar and turbulent flows into four levels and indicated that the state-of-the-art is no higher than the middle of the third level as indicated by symbol x in Table 1. At this state-of-the-art, only the problems which are suitable for a strong viscous/inviscid interaction based on the time-averaged Navier-Stokes equations with the thin boundary layer approximation can be solved with confidence. Kline, Ferziger and Johnston²³ and Chapman²⁴ discussed computational fluid dynamics (1978 and 1979 respectively). Summaries of these outlooks are presented in Tables 2 and 3.

To give some indications as to when the problem of the flows around appended bodies can be solved using the full Navier-Stokes equations, a projection by Chapman²⁴ on a similar problem in aerodynamics is worthwhile mentioning. According to him the practical 3D wing/body problem probably can be solved using the full Navier-Stokes equations by 1990's, but still at a prohibitive cost and, in addition, a more than two orders of magnitude larger computer than what is available today would be required.

The above discussion indicates that at present the attempt to predict the wake of appended bodies by solving the full Navier-Stokes equations is unrealistic.

Therefore, the survey of the numerical methods adequate for wake prediction will be confined to those associated with solving the time-averaged Navier-Stokes equations with various degrees of simplifications.

Because of the above restriction, several interesting numerical methods will not be discussed. Among them are the spectral method²⁵, the large eddy simulation with a subgrid closure²⁶ and the discrete vortex method^{27,28}. Of particular interest is the recent development of the discrete vortex method which appears to be rather attractive to simulate separated flows and wakes. For a quite different reason, the finite element method will also not be discussed. It is the author's opinion that the choice between a finite element method and a finite differential method is more of a matter of personal preference; furthermore, the finite element method is used infrequently in the computation of turbulent boundary layers. Some fundamental aspects of the finite element method in fluid mechanics are discussed by Shen²⁹.

Thus, the numerical approaches to be surveyed are finite differential methods and momentum integral methods based on the simplified Navier-Stokes equations. When the thin boundary layer approximation is used, or even when this approximation is relaxed, the pressure distribution needs to be provided in order to initiate boundary layer calculations. This pressure distribution is normally provided by the potential flow calculation. For this reason, calculation methods for the potential flow will also be discussed.

FINITE DIFFERENTIAL METHODS

Depending on approximations made, the governing equations can be divided into four types as shown in Table 4. The mathematical classification of the types of the governing equations can be found in Wang's paper³⁴.

From a computational point of view, the distinctions among these four types of governing equations are important. For the hyperbolic and the parabolic type of equations, the pressure field is assumed known and the velocity components can be computed by marching downstream. No iteration of solutions is needed in this calculation procedure. For the elliptic type of equations, both the pressure and the velocity components are unknowns and must be obtained by iteration of solutions, thus resulting in large demands on the computer memory and the computer cost. The complexity of the calculation procedure for the partially parabolic type is intermediate between the above two extremes. The pressure field of the entire computational domain is assumed known and the velocity components are then computed by marching downstream. Once these are done, a new pressure field is calculated from them and the calculational procedure is repeated until a convergence of the solution is obtained. Thus, unlike the elliptic type of equations, only a three-dimensional memory of the pressure is required by the partially parabolic type.

The calculation procedure for the partially parabolic type was first applied by Pratap and Spalding³² to the flow in curved ducts. The results agree with the experimental results better than those obtained by the parabolic type of equations. A further comparison of these two types of equations has been discussed by Spalding and his coworkers³⁵. Because the pressure field of the entire computational domain, including the normal pressure gradient, is considered, the use of the calculation procedure of the partially parabolic type of equations is worthy of a careful consideration for the prediction of the flows around appended bodies.

To close the time-averaged Navier-Stokes equations such that the number of equations and the number of unknowns are equal, a turbulence closure model is needed to connect the Reynolds shear stress and the mean field. Turbulence closure models

being used at present can be divided, according to the order of increasing complexity, into: zero-equation model, one-equation model, two-equation model, stress-equation model and large-eddy simulation with a subgrid scale model. Detailed discussions of these models can be found in the review papers by Reynolds³⁶ and Reynolds and Cebeci³⁷. The experience with numerical computations indicates that the use of the stress-equation model where each component of the six Reynolds shear stresses is solved by a partial differential equation is uneconomical at present in the sense that the improvement in the quality of solution is insignificant despite a considerable increase in the amount of the computational effort. The use of the large-eddy-simulation model is even more complicated. Thus, the use of the zero equation, one-equation and two-equation model appears to be worthy of further explorations for the purpose considered here, despite the deficiencies of these models.

The two most popular versions of the zero-equation model are the eddy-viscosity model and the mixing-length model. The basic assumption for both is that the local production of the turbulence energy is balanced by the dissipation of the turbulence energy. Consequently, the Reynolds shear stress is related to the mean velocity field by an algebraic equation. This model has been fully exploited by Cebeci³⁷. For complex turbulent flows, such as flows around appended bodies, the assumption that the local turbulence energy production is equal to its dissipation is not valid, and the advection and diffusion of the turbulence energy must be included in the energy budget. Therefore, a higher-order turbulence closure model may be needed. The most developed one-equation model is that proposed by Bradshaw et al³⁰ where the equation for the turbulent kinetic energy is solved for the connection between the Reynolds shear stress

and the mean field. This model has an excellent performance in the 1968 Stanford conference³⁸. For a two-equation model, not only the equation for the turbulent kinetic energy but also the equation for the dissipation, or a characteristic turbulent length scale is solved. The construction of two-equation models is currently an active research area. A critical examination of four popular two-equation models has been given in Reference 39.

As common in the numerical calculation of turbulent boundary layers, the choice of which turbulence closure model is most appropriate for the flow around appended bodies is not trivial nor clear-cut even when the physics of the problem is relatively well understood. In a recent calculation⁴⁰ of 3D boundary layers involving flow separations on practical wing configurations, despite the fact that the simple eddy-viscosity model is inadequate for the physics of the problem, the results obtained by more sophisticated models such as one-equation and two-equation models do not seem to significantly improve those obtained by using a simple eddy-viscosity model. The conclusion is that a simple turbulence model, such as the eddy-viscosity model or Bradshaw's one-equation model³⁰ should be preferred subject to modifications according to the specific physics of the problem under consideration.

MOMENTUM INTEGRAL METHODS

One of the major difficulties in the calculation of turbulent boundary layers is the specification of the Reynolds shear stress everywhere in the boundary layer. One of the main motivations of momentum integral methods is to avoid the need to

specify the Reynolds shear stress everywhere in the boundary layer except on the wall. This is done by integrating the governing equations from the wall to the edge of the boundary layer such that only the skin friction on the wall needs to be specified, which is then obtained from empirical data.

In addition to the empirical skin friction formula and the mean velocity profile including both the streamwise and the transverse (i.e. crossflow) direction, an auxiliary equation is needed. Depending on which of the following three equations - the entrainment equation⁴¹, the energy equation⁴² and the moment of momentum equation⁴³ is chosen as the auxiliary equation, momentum integral methods are divided into three families⁴⁴. Since the entrainment equation appear to be most thoroughly developed, the use of it as the auxiliary equation is recommended.

In the recent past, momentum integral methods have received severe criticisms from several people, including Wheeler and Johnston⁴⁵, Landweber⁴⁶ and Landweber and Patel⁴⁷. The main criticism is in the use of mean velocity profiles. Of particular concern is the fact that the crossflow velocity profile varies so much according to different flow problems considered that it is impossible to find a universal crossflow velocity profile which is applicable to a wide class of problems. However, if the interest is confined to a specific problem where drastic changes in flow characteristics are not expected, then the ground for the above criticism disappears. The flows around appended bodies considered here belong to this class of problems and momentum integral methods deserve a serious consideration because of their simplicity of computation and their flexibility to adjust to experimental data.

For momentum integral methods, the streamline coordinate system appears to be most adequate. As mentioned above, empirical formulas for the skin friction, the mean velocity profiles and the entrainment function are needed in these methods.

These formulas are mostly obtained from the measurements of various two-dimensional turbulent boundary layers. If the streamline coordinate system is used, the turbulent boundary layer in the streamwise direction of the free stream can be regarded as "two-dimensional" and those formulas mentioned above can be applied directly in the streamwise direction. Then the skin friction and the entrainment function in the crosswise direction can be determined once the limiting crossflow angle (i.e. the angle between the wall limiting viscous flow direction and the free stream streamwise direction) is computed from a given crossflow velocity profile. This approximation essentially reduces the additional information required by three-dimensional turbulent boundary layers to the specification of a crossflow velocity profile. The justification of the use of a two-dimensional turbulent boundary layer mean velocity profile family to represent a three-dimensional turbulent boundary layer has been critically discussed and confirmed by Cumpsty⁴⁸.

POTENTIAL FLOW METHODS

The progress in the calculation of the potential flow around an arbitrary configuration such as an aircraft has been rapid and successful in recent years. The main driving forces of the success are the use of the panel method to describe the surface of a complicated geometry and the rapid increase in recent years of the computer capacity which makes the use of the panel method feasible. For the state-of-the-art of potential flow methods, one is referred to the papers by Hess⁴⁹ and by Carmichael and Erickson⁵⁰.

The classification of potential flow methods is non-trivial and often mathematically inconsistent. It suffices for the purpose here to divide them into zero-order methods and higher-order methods. In a zero-order method, the panel element is flat and the source distribution over it is a constant while in a

higher-order method, either the panel element is not flat or the source distribution is not a constant, or both. The XYZPF computer program used at DTNSRDC is a zero-order method based on a theory developed by Hess and Smith (cf. Hess⁴⁹). In this method, the panel element is a flat quadrilateral and the source strength is constant. The theory developed by Webster⁵¹ is a higher-order method where the source strength over it is distributed as a linear function of position over the panel element which is a flat triangle. The most developed higher-order method is the PAN AIR computer program discussed in Reference 50.

The main short comings of the zero-order method such as the one used in the XYZPF program, are that the source distribution is discontinuous between panels resulting spurious vortex sheets and that leakage occurs between panels because flat trapezoids cannot properly cover a strongly curved surface, such as the nose or the tail portion of an ellipsoid. It is possible, that by increasing the number of panels the difficulties mentioned above may disappear, at least partially. However, for a configuration with a complicated geometry such as the one under consideration, the number of panels may not be allowed to increase to a desirable level because of the limitation in the computer storage. Thus, for the problem considered here, a higher-order method is recommended.

There is a further consideration which also favors the use of a higher-order method. When a simplified version of the Navier-Stokes equations, such as the parabolic type, is used to solve complex turbulent flows, an adequate scheme of the viscous/inviscid interaction is essential for obtaining adequate solutions. As discussed above, the complex flow field around an appended body includes flow reversals in the streamwise and the transverse direction, both driven by pressure forces. Since the ellipticity of the flow has been eliminated by the

parabolization of the governing equations, the only mechanism by which downstream conditions can influence upstream stations is through the pressure distribution which is calculated by the potential flow method. Thus, accurate potential flow calculations are crucial in obtaining viscous flow solutions and a higher-order calculation method for the potential flow appears to be more adequate.

COMPARISON OF NUMERICAL METHODS

In several international conferences, some test cases with experimental data were set up and researchers with numerical codes were invited to perform computations on the test cases; the computational results were then compared and the numerical methods evaluated. Table 5 provides a list of six major conferences with brief comments on the findings; the emphasis here is on the comparison between finite differential methods and momentum integral methods.

Of particular interest is the computation of the flow induced on a flat plate by a circular cylinder based on the experimental data of East and Hoxey¹⁰. It is considered a reasonable goal of the current state-of-the-art of three-dimensional turbulent boundary layer calculation methods to predict the separation line. Yet, none of the methods presented by the participants was capable of doing this in 1975 (cf. East⁵²). The calculation of one of the test cases in the 1980-81 Stanford Conference⁵⁶ on the junction flow in an idealized wing/body combination based on the experiment by Shabaka and Bradshaw¹³ (cf. Figures 11a and 11b) is also of interest. However, the result of evaluation is not available at the time of this writing.

A general conclusion on the comparison of finite differential methods and momentum integral methods can be derived from the results of the conferences listed in Table 5. Despite the potential advantage of finite differential methods in the

computation of more complex flow problems, such an advantage has not been demonstrated in general validity at present; momentum integral methods continue to perform as well as finite differential methods in all classes of flow problems tested including those with flow separations. As concluded in the preliminary Evaluation Committee Report of the 1980-81 Stanford Conference based on the various test problems considered, momentum integral methods continue to perform adequately and for engineering purposes are sufficient and sometimes preferable.

NUMERICAL TREATMENT OF MAIN FLOW FEATURES RELEVANT TO APPENDED BODIES

If tail fins are attached to the axisymmetric body of revolution shown in Figure 1 at a location approximately 95 percent of the total length downstream of the nose of the body, then the tail fins will be immersed in the thick turbulent boundary layer as mentioned earlier. The main flow features in the boundary layer and the wake of the tail-fin/body combination can be summarized as: thick turbulent boundary layer, two-dimensional and three-dimensional flow separation, secondary flow and wake. The wakes of tail fins will interact with the boundary layer of the body. However, this interaction is unlikely to be important since the boundary layers on tail fins are expected to be small compared to that on the body.

THICK TURBULENT BOUNDARY LAYER

The streamwise vortex motion in the junction flow of a fin/body combination depends on the strength and the size of the horseshoe vortex generated in the leading edge of the fin/body combination. Since the strength and the size of the horseshoe vortex depends on the thickness and the mean velocity profile of the incident turbulent boundary layer, an accurate prediction of the thick turbulent boundary layer is essential for wake prediction.

The main difficulty in the calculation of the thick turbulent boundary layer arises due to the approximation made that the normal pressure variation across the boundary layer is zero in order to simplify the Navier-Stokes equations. Thus, if no approximation is made the difficulty does not arise, but then the pressure must be calculated simultaneously with velocity components. On the other hand, if the pressure is assumed to be constant across the boundary layer, the equations are simplified to the parabolic or the hyperbolic type, but then, an adequate viscous/inviscid interaction scheme is necessary to account for the correction due to the normal pressure variation across the boundary layer.

Major methods used for the numerical treatment of the thick boundary layer are listed in Table 6. The order of listing is according to the decreasing degree of demand on computing efforts. Representative references are also given for each method.

As mentioned earlier in the experimental aspect of the thick turbulent boundary layer, the structure of turbulence is different from that of a flat plate. Since most of turbulence closure models are constructed based on the data obtained in flat plates, modifications are needed when applied to thick turbulent boundary layers. In the simple mixing-length model used by Wang and Huang⁵⁹, such modifications have been made. The question of whether modifications are needed in two-equation turbulence models does not appear to have received attention.

The approach adopted by Wang and Huang in making correction to the mixing length in the region of the thick boundary layer is solely based on experimental data. A more rational approach has been suggested by Bradshaw^{62,63}. As mentioned earlier, the thick boundary layer normally occurs in the region where the surface

curvature along which the flow travels is relatively large. In the case of the axisymmetric body of revolution, this region occurs near the stern where the longitudinal surface curvature is large. Bradshaw proposed that the change in the structure of the turbulent boundary layer be accounted for by making correction to the dissipation length scale due to the extra strain introduced by the effect of the streamline curvature. This idea has been applied by Patel and Lee⁶⁴ to the body of revolution using a finite differential method with Bradshaw's one-equation model³⁰. A similar application, but, using the momentum integral method has been done by Green, Weeks and Brooman⁶⁵.

A new development to account for the normal pressure variation across the boundary layer using momentum integral methods is proposed by Le Balleur⁶¹. The departure of this approach from the classical one is that the viscous and inviscid equations are solved simultaneously in the boundary layer with the boundary condition of the inviscid flow on the wall determined by the surface transpiration method. The ingenuity of this approach is that the pressure in the boundary layer is set equal to that of the inviscid flow in the first-order approximation when curvature effects are neglected. Since at high Reynolds numbers, the experimental evidence indicates that the actual pressure distribution is very close to that of the inviscid flow, this approach allows for a variation in the normal pressure across the boundary layer while solving the same set of the governing equations used in the thin boundary layer approximation. The disadvantage of this approach is that the various boundary layer thicknesses are defined based on the inviscid flow velocity on the wall rather than on the edge of the boundary layer. Therefore the application of the empirical formulas which have various boundary layer thicknesses as parameters requires modifications. Fast⁶⁶ has extended the theory to include the second-order effects due to surface curvatures

in two-dimensional problems. The extension to three-dimensional problems has not been made, but it is feasible.

FLOW SEPARATION

Two types of flow separation occur in the flow field as shown in Figure 5. The separation point upstream of the leading edge of the appendage is a two-dimensional singularity with zero skin friction; but the separation line which encircles the appendage like a necklace is not a line of singularities, rather, it is a line along which the limiting wall streamlines converge. Thus, numerically, the first type of separation creates much more difficulty than the second type.

Since the skin friction approaches zero, a natural criterion for the prediction of the singular separation point is to locate the point where the skin friction is zero. However, it has been found that numerically it is easier to locate this point approximately as where the displacement thickness increases sharply. To numerically march across the singular separation line, the so called inverse mode is used. In the inverse mode, the displacement thickness is specified and the pressure gradient predicted; this is contrary to the usual direct mode where the pressure gradient is specified and the displacement thickness predicted. A clear illustration that the singularity in the governing equations is removed by using the inverse mode is given by Cousteix and Houdeville⁶⁷. Other applications of the inverse mode to calculate separated flows using momentum integral methods are discussed by Cousteix et al⁶⁸, East et al⁶⁹, Whitfield et al⁷⁰ and Stock⁴³. Similar applications using finite differential methods are discussed by Catherall and Mangler⁷¹, Carter⁷² and Formery and Delery⁷³.

The paper by Formery and Delery is of particular interest. They assumed that the pressure is constant in the direction normal to the wall but is allowed to

vary in the transverse direction and succeeded in calculating the flow field in the vicinity of the separation line in the experiment of East and Hoxey¹⁰ as shown in Figure 12. They did not attempt to calculate the entire region of the horseshoe vortex motion (i.e. region (1) in the previous discussion) and probably would have failed since the elliptic type of the governing equations must be used in this region. Some attempts^{74,75} to calculate the flow field in this region have been limited to low Reynolds numbers in the range of 100-500.

Since the pressure force is the dominant driving force in this region, the governing equations chosen must allow for pressure variations in all three dimensions or a strong viscous/inviscid interaction scheme must be used to account for pressure variations via potential solutions which are elliptic. On the other hand, because the pressure is the dominant force, Reynolds shear stresses are less important and a simpler turbulence closure model may be adequate as is suggested by the calculation of Formery and Delery.

SECONDARY FLOW

The term secondary flow is used here to indicate the flow field with a significant component of crossflow due to the geometry. This flow field includes region (2) of the junction flow with a strong streamwise vorticity and region (3) of the large crossflow region. The latter region includes the crossover (or S-shaped) crossflow in the vicinity where the free-stream streamline has a point of inflection and the non-crossover crossflow in the upstream and the downstream portion of the point of inflection. Unlike region (1) where the horseshoe vortex is generated, the flow reversal in the streamwise direction does not take place in regions (2) and (3). Calculations made by Pratap and Spalding³² indicate that a partially parabolic type of equations will be adequate in these flow regions.

The experiment by Shabaka and Bradshaw¹³ indicates that the direction of the velocity gradient vector differs significantly from that of the shear stress in the junction flow. This implies that the simple eddy-viscosity and the mixing-length turbulence models may not be adequate in this region, although the contrary is indicated earlier⁴⁰. Numerical calculations of the junction flow in a wing/body combination are not available at present except some attempts in laminar flows^{8,74,76}. However, some calculations will appear in the 1980-81 Stanford Conference⁵⁶.

Although the origin of the corner flow⁷⁷ is Reynolds-shear-stress-driven and is different from the junction flow considered here, the basic flow features have some similarities and the numerical calculations^{78,79} of the corner flow can provide helpful information.

If momentum integral methods are attempted, then the mean velocity profiles, particularly in the crosswise direction, must be constructed based on experimental data such as the secondary flow vectors shown in Figure 11b. No such attempt has been made at present. According to the experimental evidence¹³, the strength of the streamwise vortex decreases and the size increases downstream due to the diffusion of the Reynolds shear stresses. This diffusion effect and the mean velocity profiles are the main features that need to be considered in the modeling of the junction flow.

Relatively abundant and successful calculations have been performed in the flow fields relevant to region (3) where the non-crossover crossflow is important. However, when crossover of the crossflow occurs, numerical calculations encounter difficulties and in general the results are not satisfactory⁵⁵. A review of the numerical methods by finite differential approaches with emphasis on turbomachinery has been given by McNally and Sockol⁸⁰. A parallel review based on momentum integral approaches has been given by Horlock and Perkins⁸¹.

Because of its simplicity, the momentum integral approach is attractive in this flow region. The most popular crossflow models are those by Mager and Johnston and those using polynomials. For a general discussion of these models, one is referred to Reference 11. A comparison of the results obtained by using the Mager and the Johnston model has been made by Myring⁸². It is found that because the Johnston's model includes a Reynolds number dependency, it leads to a better agreement with the experiment than the Mager's model at high Reynolds numbers. However, comparisons made by Smith⁸³ on several experiments have not indicated superiority of either model. Because of the rather artificial requirement of satisfying the boundary conditions at the wall and the edge of the boundary layer in order to determine the coefficients of the polynomial, the polynomial model does not appear to be general. At present, the attempts to include the S-shaped cross flow have only produced a qualitative agreement with the experiment at best. Some discussions of this subject are given in References 11 and 84-86.

WAKE

It is known that Reynolds shear stresses play important roles in the rapidly relaxing turbulent flow in near wakes. A review of two-dimensional experimental data and prediction methods has been given by Patel and Scheuerer⁸⁷. They also evaluated the use of the $\kappa-\epsilon$ turbulence closure model, and found that while the results in near wakes are reasonable, the results in far wakes are not in satisfactory agreement with experimental data. The techniques used in the prediction of near wakes of airfoils are a good source to search for a suitable method. Some current reviews of the subject are given by Lock⁸⁸, Look and Firmin⁸⁹, Melnik⁹⁰ and Le Balleur et al.⁹¹

Some simpler approaches to predict near wakes are of interest. For a body of revolution, Wang and Huang³⁴ use a polynomial to connect the stern boundary layer region and the far wake region while Nakayama et al⁵⁸ enforce the conservation of momentum in the longitudinal direction. The treatment of wakes using a momentum integral method has been discussed by Green⁹², and subsequently improved by Green et al⁶⁵. In this method, the governing equations in the wake are the same as in the boundary layer except that the skin friction is set equal to zero since there is no wall boundary and the dissipation length scale is doubled in order to match the behavior in the far wake.

SUMMARY AND RECOMMENDATION

Due to the limitation of computer capability, solving the time-dependent full Navier-Stokes equations for the purpose of the wake prediction of submerged appended bodies is not feasible at present. Even when time dependency is eliminated by the time-averaging method, the governing equations are of the elliptic type and the computing effort for the problem considered here is still too enormous to be practical. Therefore, further simplifications must be made. For example, the diffusion of momentum in the predominant flow direction can be neglected such that the elliptic type is simplified to the partially parabolic type; or the thin boundary layer approximation supplemented by viscous/inviscid interaction can be made. Once the type of the governing equations, the turbulence closure model and the calculation method of the potential flow have been chosen, the numerical method can proceed according to either the finite differential approach or the momentum integral approach.

If the finite differential approach is followed, then the partially parabolic type of the governing equations and a turbulence closure model no more complicated

than the $\kappa-\epsilon$ model are preferred. Numerical experiments indicate that the partially parabolic type of the governing equations supplemented by the $\kappa-\epsilon$ model will likely be adequate for the flow regions dominated by the streamwise vortex motion (region(2)) and by the crossflow (region (3)). However, its adequacy in the region where flow reversal in the predominant flow direction occurs, i.e. region (1) where the horseshoe vortex is generated, is uncertain. If the latter method is adopted, then the generality of the finite differential approach will be limited to the class of problems where the experimental data used are applicable.

The major shortcoming in the use of the momentum integral approach to three-dimensional flow problems is the fact that the mean velocity profile in the crossflow direction varies significantly from one flow problem to the other, and an adequate similarity law of the mean velocity profile in the crossflow direction applicable to a large class of flow problems has yet to be found. However, if the aim of the application is not universal, but is confined to the special class of flows around appended bodies of limited geometrical variations, then the more empirically-oriented momentum integral approach will most likely be adequate. The continued usefulness of momentum integral approach to three-dimensional flow problems has been demonstrated in several recent international conferences where finite differential methods and momentum integral methods were compared and evaluated. If the momentum integral approach is adopted for the wake prediction of submerged appended bodies, then the main task will be to construct the empirically based models of mean velocity profiles appropriate for the three flow regions mentioned above.

The choice of a numerical method is in general based on the consideration of generality versus practicality and accuracy versus efficiency. There is a common agreement that finite differential methods tend to be more general and to provide more accurate and detailed solutions, or have the potential to do so; while momentum integral methods are less general, and are only capable of providing solutions of global flow features. On the other hand, momentum integral methods are much simpler; therefore are computationally more efficient and are practical for many engineering applications. It has been mentioned above that the elliptic type of governing equation is adequate for the problem considered here, but the computational cost and effort are prohibitive at present. If the simpler partially parabolic type of governing equation is adopted, then it is likely that the computational difficulties in thick turbulent boundary layers and large cross flows can be overcome. However, the capability of the partially parabolic type equations in computing the flow region where the horseshoe vortex is generated has not been demonstrated.

From the above discussions, it appears that at the present time, there is no adequate method which is capable of computing the wakes of submerged appended bodies in a complete fashion, and at the same time, meeting the criteria of both generality and accuracy of the solution. For this reason, two approaches are recommended to be pursued simultaneously. One approach is for immediate applications and the other approach for long-range research. For the first approach, the momentum integral method is recommended due to its relative simplicity and its flexibility to adapt to experimental data. For the second approach, a numerical procedure no less sophisticated than the one by solving the partially parabolic Navier-Stokes equations with the $\kappa-\epsilon$ turbulence model should be considered.

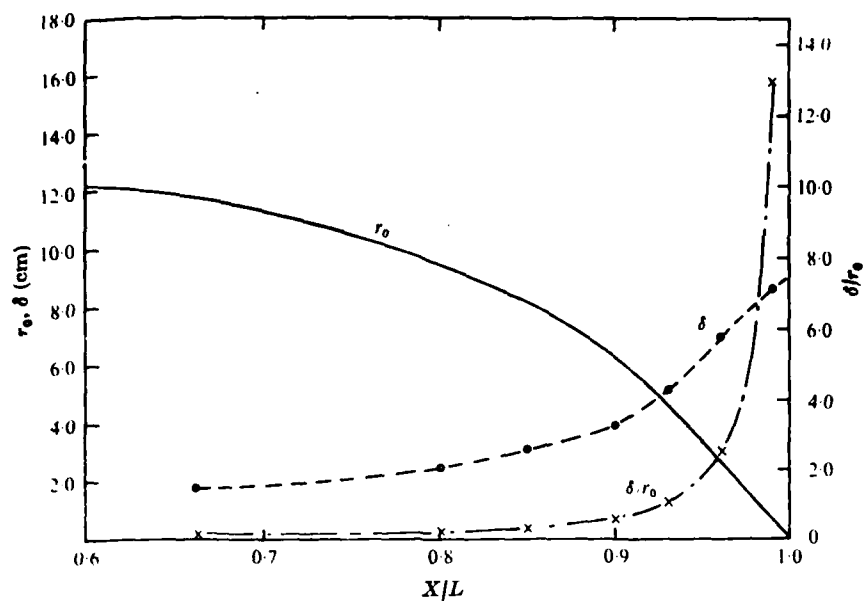


Figure 1 - Variation of Boundary-Layer Thickness and Local Radius of the Body (Taken from Reference 1)

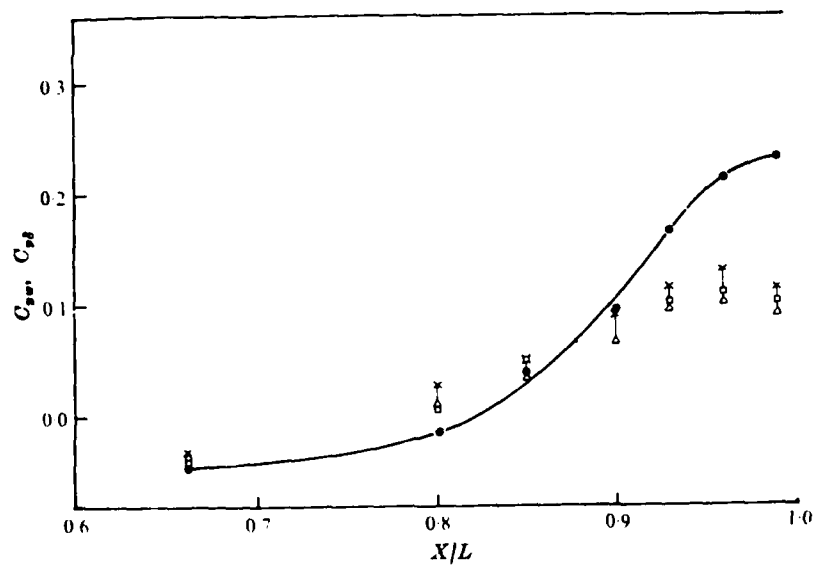


Figure 2 - Variation of Wall Static Pressure and Total Pressure at the Edge of the Boundary Layer.

•, C_{pw} (Wall Static Pressure); x, $C_{p\delta}$ (Total Pressure; Single Wire); □, $C_{p\delta}$ (Total Pressure; Static Tube); Δ, $C_{p\delta}$ (Total Pressure; Bernoulli Equation)
(Taken from Reference 1)

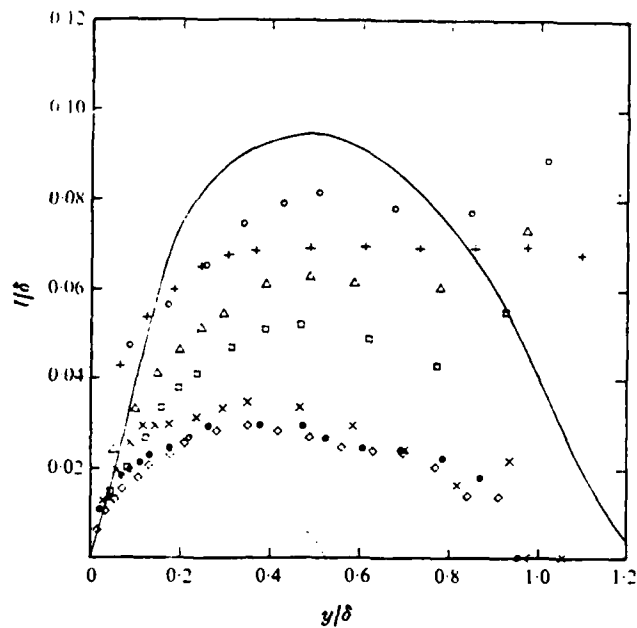


Figure 3 - Mixing-length Profiles —, Bradshaw et al.
(Thin Boundary Layer). (Taken from Ref. 1)

	○	+	△	□	×	◇	◇
X/L	0.662	0.80	0.85	0.90	0.93	0.96	0.99

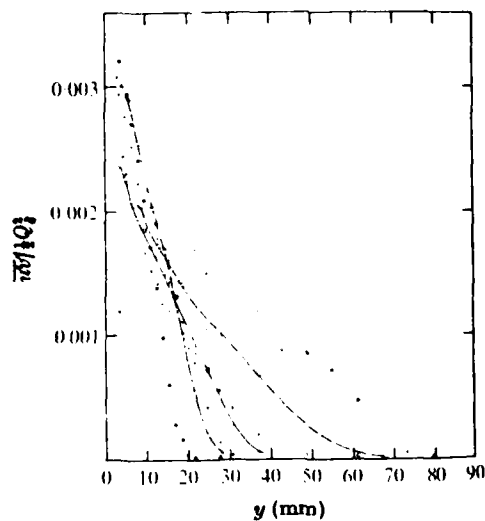


Figure 4 - Variation of Axial Reynolds Shear Stress
(Taken from Reference 1)

	●	▽	+	□	×	△	○
X/L	0.662	0.80	0.85	0.90	0.93	0.96	0.99

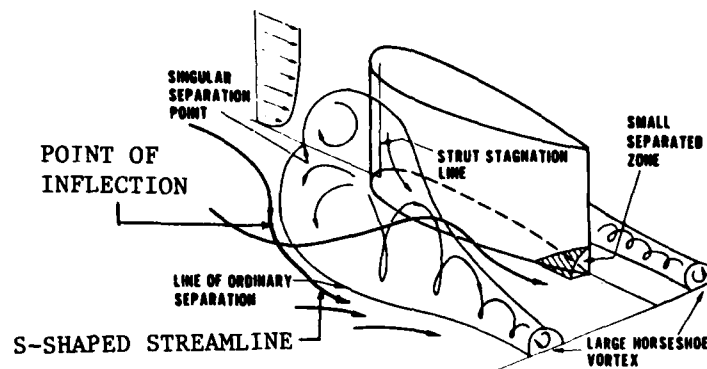


Figure 5 - Flow Field of the Appendage/Body Junction (Taken from Reference 5)

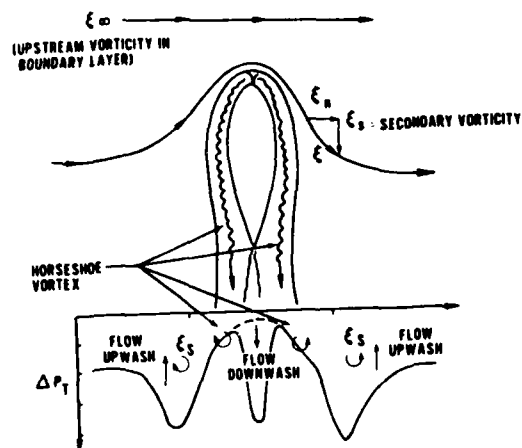


Figure 6 - Wake of the Appendage/Body Junction Induced Flow Field (Taken from Reference 5)

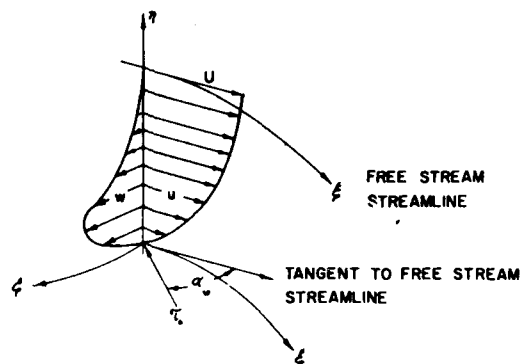


Figure 7 - Non-Crossover Type of Crossflow
(Taken from Reference 11)

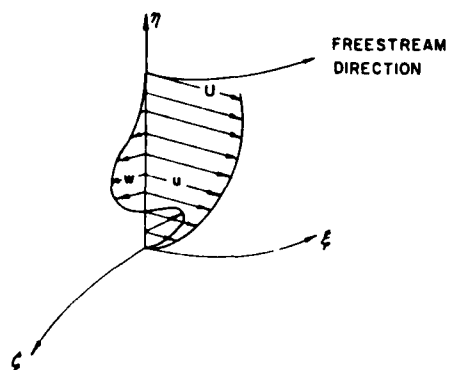


Figure 8 - Crossover (or S-shaped) Type of Crossflow
(Taken from Reference 11)

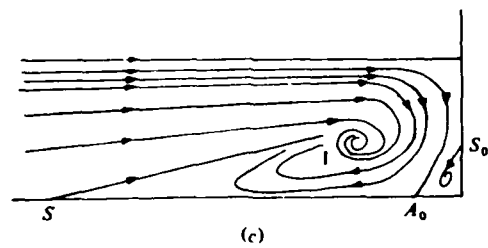
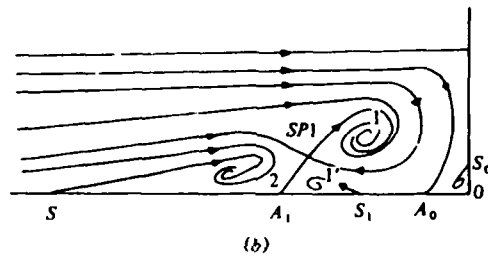
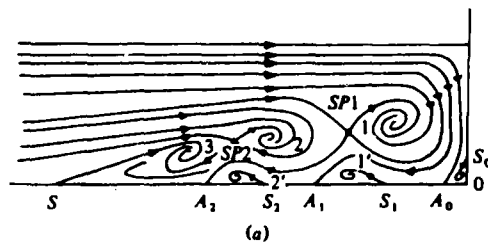


Figure 9 - Streamline Patterns of Horseshoe Vortices (Laminar Flow):
 (a) Six Vortex System; (b) Four Vortex System; (c) Two Vortex System. S, Separation Line; A, Attachment Line; SP, Stagnation Point. (Taken from Reference 7)

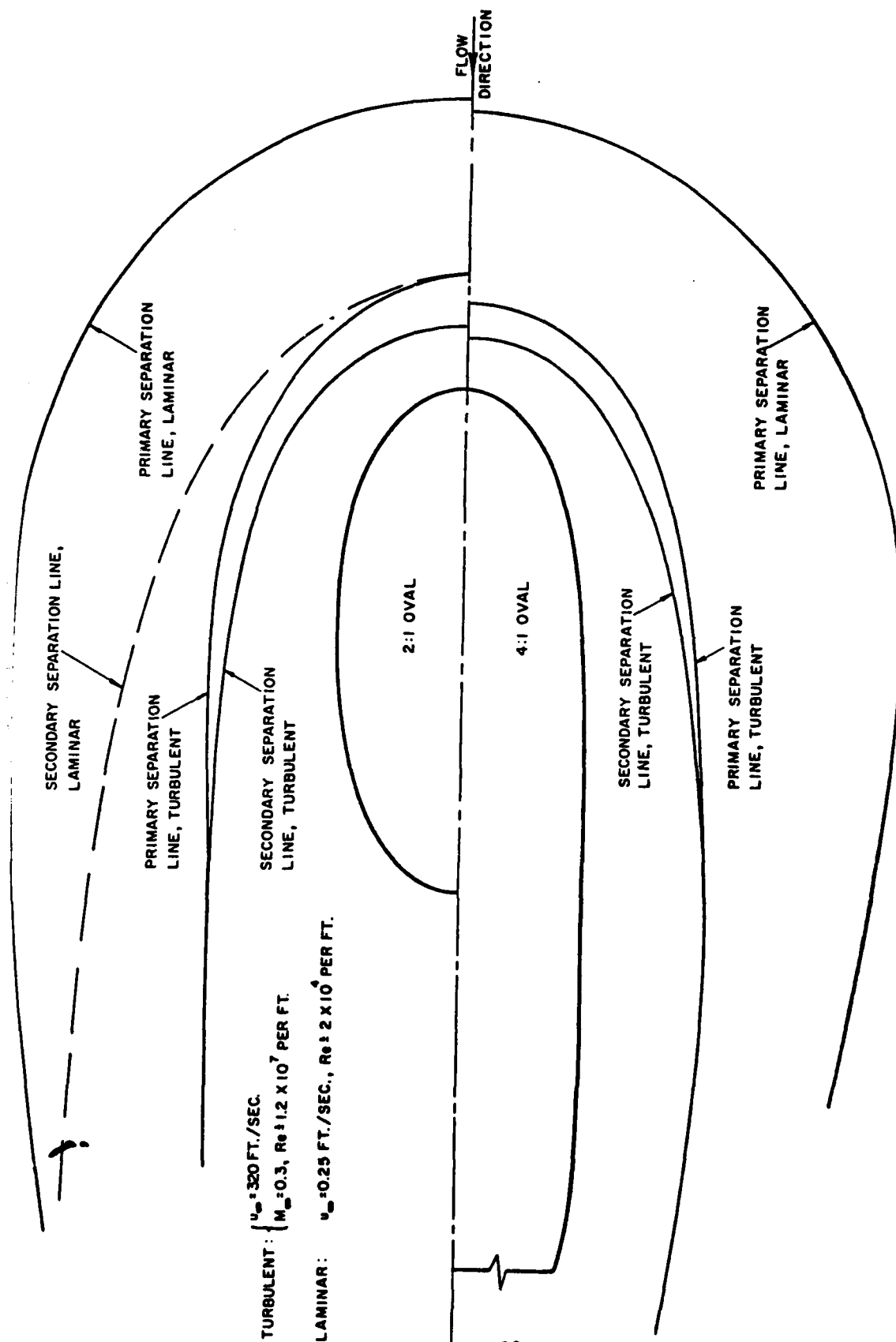


Figure 10 - Comparison Between Experimental Laminar and Turbulent Flows About 2:1 and 4:1 Ovals (Taken from Reference 10)

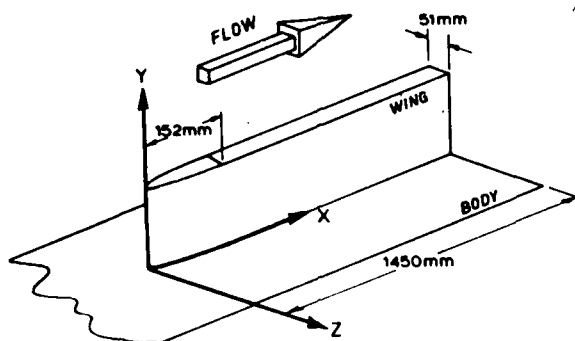


Figure 11a - Idealized Wing/Body Junction
(Taken from Reference 13)

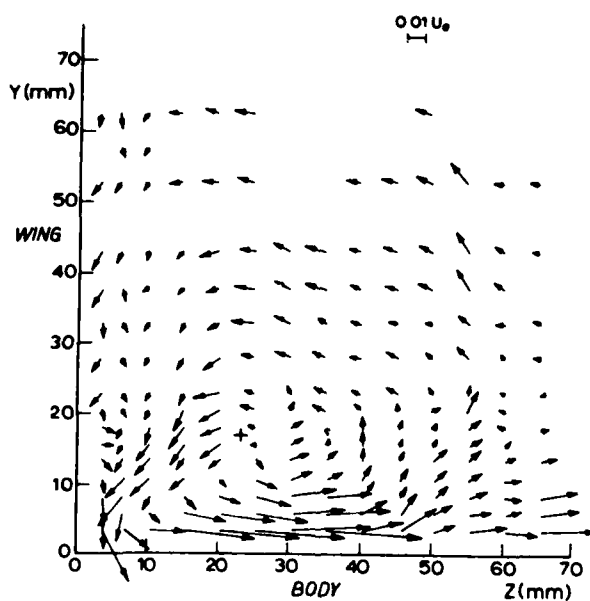


Figure 11b - Secondary Flow Vectors at a Downstream Station
 $X=1223$ mm of the Idealized Wing/Body Junction

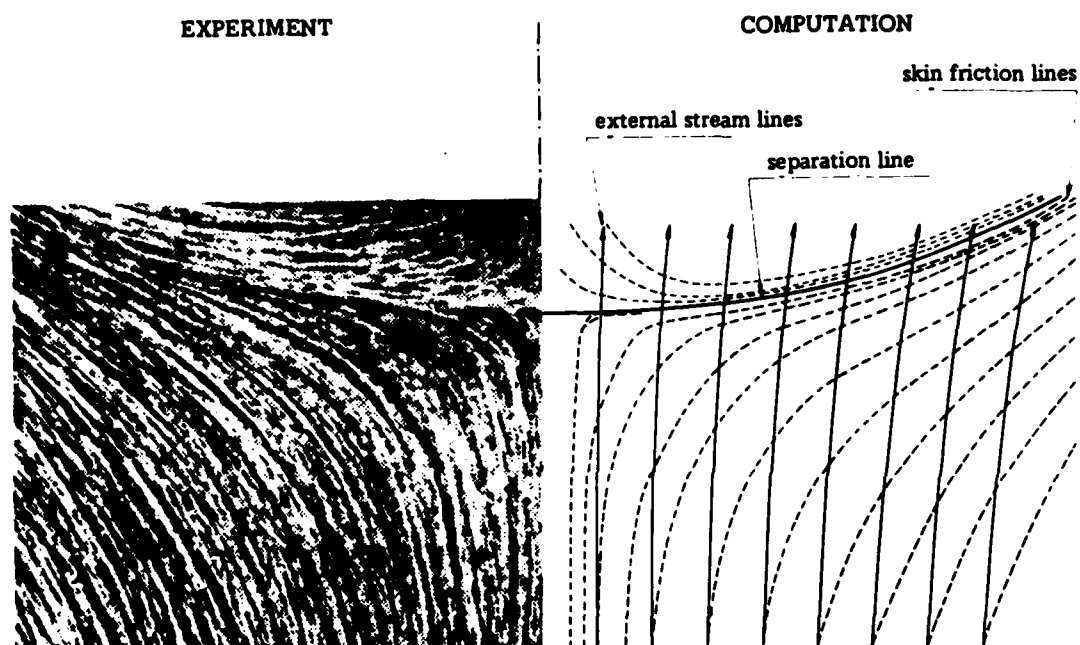


Figure 12 - Comparison of Experiment and Computation of the Separation Line in Front of the Cylinder/Flat-Plate Junction¹⁰ (Taken from Reference 76)

TABLE 1

Levels of Approximation and the State-of-the-Art of
Computational Fluid Dynamics
(Taken from Reference 22, 1980)

Level of Approximation	State-of-the-Art
1 - Ideal fluid	
2a - Ideal fluid + nondimensional empirical correlations	
2b - Ideal fluid + boundary layers (weak coupling)	x
2c - Parabolized approximations of the Navier-Stokes equations	x
2d - Ideal fluid + isobaric separated zones	x
3a - Ideal fluid + thin viscous layers (strong coupling)	x
3b - Ideal fluid + Navier-Stokes zones (strong coupling)	
4 - Direct overall solutions of the Navier-Stokes equations:	
4a - Averaged equations + turbulence model	
4b - Filtered equations (simulation of the large turbulent structures)	
4c - Complete equations (numerical simulation of turbulence).	

TABLE 2
Status and Outlook of Computational Fluid Dynamics
(Taken from Reference 23, 1978)

Level	Example	Comments
1. Nondimensional correlation of data.	f versus Re for pipe flow; C_p as a function of geometry for straight-walled diffusers; C_D versus Re for flow normal to cylinders, over spheres, etc.	Slow, expensive, accretive; high reliability within carefully defined class of flow situation.
2. Zonal models.	(a) Conventional boundary layer theory for attached flows, matched to external flow via *. (b) Hyper-boundary layer inviscid zonal models, for strong interactions such as detaching flows.	The major class of engineering solutions currently. Advancing rapidly, good promise for many more classes of practical solutions and design tools by 1988. Computing costs well within engineering feasibility. A number of research groups currently active.
3. Numerical solutions for Reynolds equations (time-averaged Navier-Stokes equations).	A number of codes now exist. Can be used for part of flow and matched to external flow like 2b or over entire field.	Also advancing rapidly. To date methods don't appear to extrapolate well; as in Class 2 need to be fitted to specific classes of flows.
4. Large eddy simulation with subgrid closure.	Current research - few solutions yet available.	Computing costs still relatively high. Outcome highly dependent on further advances in large computers.
5. Complete solutions to Navier-Stokes equations	(a) Analytic. A dozen or so closed solutions (for very simple cases) exist as the results of 150 years work. (b) Numerical. Only the very simplest cases, which have few applications, so far accessible via numerical methods.	New solutions likely to be scarce, slow; restricted to laminar flows. All but these simplest cases at very modest Reynolds numbers still too large for existing computers; progress dependent on rate of growth of computers and decrease in computing costs.

TABLE 3

Development of Computational Aerodynamics
(Taken from Reference 24, 1979)

Stage	Readiness Time Period				Computer Class for Practical 3-D Calculations
	Computer Results	2-D Airfoil	Simple 3-D Wing	Simple 3-D Wing-Body	
I Linearized inviscid	Pressure distribution Vortex drag Supersonic wave drag	1930	1940's	1968	IBM 360 CDC 6600
II Nonlinear inviscid	Above plus: Transonic flow Hypersonic flow	1971	1973	1976	Current supercomputers
III Navier-Stokes Re-averaged Model all scales of turbulence	Above plus: Separated flow Total drag Performance Buffeting, buzz	1975	1978	Early 1980's	40 x current supercomputers
IV Large eddy simulation Model subgrid- scale turbulence	Above plus: Aerodynamic noise Transition Surface pressure fluctuations	Early 1980's	Mid 1980's	1990's	At least 100 x NASF

TABLE 4

Classification of the Governing Equations

Type of Equations	Approximations	Flow Problems Solved
Hyperbolic ³⁰	Thin boundary layer and no diffusion	Flows with a predominant direction; no vortex motion
Parabolic ³¹	Thin boundary layer	Same as above
Partially parabolic ³²	Diffusion in the stream- wise direction neglected	Curved duct flows. Some degree of thick boundary layer
Elliptic ³³	No or few approximations	Horseshoe vortex and thick boundary layer

TABLE 5
Comparison of Numerical Methods

Major Editor (year)	Type of Problem	Numerical Methods		Comments
		Differen- tial	Integral	
Kline ³⁸ (1968)	33 test cases; mostly 2-D turbulent boundary layers	9	20	Of 7 in the top class, 4 are momentum integral methods and 3 are finite differential methods.
East ⁵² (1975)	7 test cases, some with separation	6	3	Momentum Integral methods have impressive, if not better performances.
Humphrey ⁵³ (1978)	A 3-D wing	5	3	Despite the fact that the flow is not strongly 3-D, the computed results scatter by as much as 20%; no preference to either numerical method indicated.
Lindhout ⁵⁴ (1979)	A 3-D wing with separation in the root section	5	4	The potential capability of finite differential methods has not been demon- strated. Momentum integral methods appear to provide more consistent results.
Larson ⁵⁵ (1980)	2 test cases of 3-D Ship boundary layers	7	10	Both finite differential and momentum integral methods failed to obtain adequate solutions in the thick turbulent boundary layer near the stern.
Kline ⁵⁶ (1980-81)	66 test cases of computer turbulent flows	A total of 73 different methods		Both finite differential and momentum integral methods are well worthy of further study and refinement.

TABLE 6*

Methods to Account for Thick Turbulent Boundary Layers

Methods	Comments	References
1. Elliptic equations	Computer cost prohibitive; not practical	Phoenics Code ³³
2. Partially parabolic equations	Iterative marching integration scheme. The rate of convergence of solution depends strongly on the quality of the initial guess on pressure	Abdelmequid et al ³⁵
3. Pressure iteration	2-D method has been developed	Mahgoub & Bradshaw ⁵⁷
4. Viscous/inviscid matching at the height of the boundary layer	An application to axisymmetric bodies of revolution has been considered	Nakayama et al ⁵⁸
5. Viscous/inviscid matching at the height of the displacement thickness	Less accurate than the above method	Wang & Huang ⁵⁹
6. Vortex Method	The tail region of the body of revolution is calculated by the vorticity equation	Geller ⁶⁰
7. Strong surface transpiration method	The pressure of the real flow is set equal to that of the inviscid flow inside the boundary layer in the first-order approximation	Le Balleur ⁶¹

*The order of listing is according to the decreasing degree of demand on computing efforts.

APPENDIX A

ALPHABETICAL BIBLIOGRAPHY OF THE LITERATURE SURVEYED

1. Abdelmeguid, A.M., N.C. Markatos, and D.B. Spalding, "A Method of Predicting Three-Dimensional Turbulent Flows Around Ships' Hulls," International Symposium on Ship Viscous Resistance, SSPA Goteborg, pp. 3.1-3.24 (1978).
2. Abdelmeguid, A.M., N.C. Markatos, K. Muraoka, and D.B. Spalding, "A Comparison between the Parabolic and Partially-Parabolic Solution Procedures for ThreeDimensional Turbulent Flows Around Ships' Hulls," Applied Mathematics Modeling 3, pp. 249-258 (1979).
3. Arnal, D. and J. Consteix, "Subsonic Flow in a Corner," La Recherche Aerospatiale 1981-1982, pp. 45-62 (1981).
4. Baker, C.J., "The Laminar Horseshoe Vortex," Journal of Fluid Mechanics, 95, pp. 347-367 (1979).
5. Barber, T.J., "An Investigation of Strut-Wall Intersection Losses," Journal of Aircraft, 15, pp. 676-681 (1978).
6. Beam, R.M. and R.F. Warming, "An Implicit Factored Scheme for the Compressible Navier-Stokes Equations," AIAA Journal, 16, pp. 393-402 (1978).
7. Belik, L., "The Secondary Flow About Circular Cylinders Mounted Normal to a Flat Plate," Aeron Quart. 24, pp. 47-54 (1973).
8. Bradshaw, P., "The Analogy between Streamline Curvature and Buoyancy in Turbulent Shear Flow," Journal of Fluid Mechanics, 36, pp. 177-191 (1969).

9. Bradshaw, P., "Effects of Streamline Curvature on Turbulent Flow," AGARD-AG169 (1973).
10. Bradshaw, P., "Calculation of Three-Dimensional Turbulent Boundary Layers," Journal of Fluid Mechanics, 46, pp. 417-445 (1971).
11. Bradshaw, P., "Review - Complex Turbulent Flows," Transactions of ASME, Journal of Fluids Engineering, 97, pp. 146-154 (1975).
12. Bradshaw, P., "Structure of Turbulence in Complex Flows," AGARD-LS-94: Three-Dimensional and Unsteady Separation, pp. 10.1-10.7 (1978).
13. Bradshaw, P., "Prediction of Separation Using Boundary Layer Theory," in AGARD-LS-94: "Three-Dimensional and Unsteady Separation", pp. 11.1-11.8 (1978).
14. Bradshaw, P., D.H. Ferriss, and N.P. Atwell, "Calculation of Boundary-Layer Development Using the Turbulent Energy Equation," Journal of Fluid Mechanics, 28, pp. 593-616 (1967).
15. Bragg, G.M., "The Turbulent Boundary Layer in a Corner," Journal of Fluid Mechanics, 36, pp. 485-503 (1969).
16. Briley, W.R. and H. McDonald, "Solutions of Multidimensional Compressible Navier-Stokes Equations by a Generalized Implicit Method," Journal of Computational Physics, 24, pp. 372-397 (1977).

17. Briley, W.R. and H. McDonald, "On the Structure and Use of Linearized Block Implicit Schemes," *Journal of Computational Physics*, 34, pp. 54-73 (1980).
18. Briley, W.R. and H. McDonald, "Analysis and Computation of Viscous Subsonic Primary and Secondary Flows," *AIAA, Computation of Fluid Dynamics Conference*, pp. 74-88 (1979).
19. Briley, W.R. and H. McDonald, "Computation of Three-Dimensional Horseshoe Vortex Flow Using the Navier-Stokes Equations," *7th International Conference on Numerical Methods in Fluid Dynamics, Stanford University and NASA/Ames* (23-27 June 1980).
20. Brown, S.N. and K. Stewartson, "Laminar Separation," *Ann. Review of Fluid Mechanics*, 1, pp. 45-72 (1969).
21. Brune, G.W., P.E. Rubbert, and C.K. Forester, "The Analysis of Flow Fields with Separation by Numerical Matching," *AGARD-CP-168: Separation in Flows*, pp. 16.1-16.8 (1975).
22. Carmichael, R.L. and L.L. Erickson, "PAN AIR - A Higher Order Panel Method for Predicting Subsonic or Supersonic Linear Potential Flows about Arbitrary Configurations," *AIAA 81-1255* (June 1981).
23. Carter, J.E., "A New Boundary-Layer Inviscid Interaction Technique for Separated Flow," *AIAA Computational Fluid Dynamics Conference, Paper 79-1450*, pp. 45-55 (1979).

24. Carter, J.E. and S.F. Wornom, "Solutions for Incompressible Separated Boundary Layers Including Viscous-Inviscid Interaction," in Aerodynamic Analyses Requiring Advanced Computers, Part I, NASA SP-347, p. 125-150 (1975).
25. Catherall, D. and K.W. Mangler, "The Integration of the Two-Dimensional Laminar Boundary-Layer Equations Past the Point of Vanishing Skin Friction," Journal of Fluid Mechanics, 26, pp. 163-182 (1966).
26. Cebeci, T., "Laminar and Turbulent Incompressible Boundary Layers on Slender Bodies of Revolution in Axial Flow," Transactions of ASME, Series D, Journal of Basic Engineering, 92, pp. 545-550 (1970).
27. Cebeci, T., K.C. Chang, and K. Kaups, "A General Method for Calculating Three-Dimensional Laminar and Turbulent Boundary Layers on Ship Hulls," 12th Symposium on Naval Hydrodynamics, Washington, DC, pp. 188-208 (1978).
28. Cebeci, T., A.A. Khattab, and K. Stewartson, "Prediction of Three-Dimensional Laminar and Turbulent Boundary Layers on Bodies of Revolution at High Angles of Attack," 2nd International Symposium on Turbulent Shear Flows, pp. 189-198 (1979).
29. Cebeci, T., K. Stewartson, and P.G. Williams, "Separation and Reattachment Near the Leading Edge of a Thin Airfoil at Incidence," AGARD-CP-291: Computation of Viscous-Inviscid Interaction," pp. 20.1-20.13 (1980).
30. Chambers, T.L. and D.C. Wilcox, "Critical Examination of Two Equation Turbulence Closure Models for Boundary Layers," AIAA Journal, 15, pp. 821-828 (1977).

31. Chapman, D.R., "Computational Aerodynamics Development and Outlook", Dryden Lecture, AIAA Journal 17, pp. 1293-1313 (1979).
32. Chorin, A.J., "Numerical Study of Slight Viscous Flow," Journal of Fluid Mechanics, 57, pp. 785-796 (1973).
33. Chorin, A.J., "Vortex Sheet Approximation of Boundary Layers," Journal of Computational Physics, 27, pp. 428-442 (1978).
34. Chorin, A.J., "Vortex Models and Boundary Layer Instability," SIAM Journal of Scientific Statistics and Computations, 1, pp. 1-21 (1980).
35. Chu, J. and A.D. Young, "Measurements in Separating Two Dimensional Turbulent Boundary Layers," AGARD-CP-168: "Separation in Flow", pp. 13.1-13.12 (1975).
36. Coles, D., "The Law of the Wake in the Turbulent Boundary Layer," Journal of Fluid Mechanics, 1, pp. 191-226 (1956).
37. Coles, D., "The Young Person's Guide to the Data," AFOSR-IFP Stanford Conference on Computation of Turbulent Boundary Layers (1968).
38. Cooke, J.C. and G.G. Breoner, "The Nature of Separation and Its Prevention by Geometric Design in a Wholly Subsonic Flow," in "Boundary Layer and Flow Control," G.V. Lachmann ed., Vol. 1, pp. 144-185 (1961).
39. Cousteix, J. and R. Houdeville, "Methode Integrale de Calcul d'une Couche Limite Turbulente sur une Paroi Courbee Longitudinalement," La Recherche Aerospatiale 1977-1, pp. 1-13 (1977).

40. Cousteix, J., J. Le Baller, and R. Houdeville, "Calculation of Unsteady Turbulent Boundary Layers in Direct or Inverse Mode, Including Reversed Flows-Analysis of Singularities," La Recherche Aerospatiale 1980-3, pp. 3-13 (1980).
41. Cousteix, J. and R. Houdeville, "Singularities in Three-Dimensional Turbulent Boundary-Layer Calculations and Separation Phenomena," AIAA Journal, 19, pp. 976-985 (1981).
42. Cumpsty, N.H., "A Critical Examination of the Use of a Two-Dimensional Turbulent Profile Family to Represent Three-Dimensional Boundary Layer," A.R.C. Current Papers 1068, pp. 37 (1970).
43. Cumpsty, N.A. and M.R. Head, "The Calculation of Three-Dimensional Turbulent Boundary Layers, Part I: Flow Over the Rear of an Infinite Swept Wing," Aeronautical Quarterly, 18, pp. 55-84 (1967).
44. Curle, N. and S.W. Skan, "Approximate Methods for Predicting Separation Properties of Laminar Boundary Layers," Aeronautical Quarterly, pp. 257-268 (1957).
45. Daiguji, H. and H. Shirahata, "The Secondary Flow about a Circular Cylinder," Bulletin of the JSME, 22, pp. 925-932 (1979).
46. Dechow, R. and K.O. Felsch, "Measurement of the Mean Velocity and of the Reynolds Stress Tensor in a Three Dimensional Turbulent Boundary Layer Induced by a Cylinder Standing on a Flat Wall," Symposium on Turbulent Shear Flow, Pennsylvania State University, pp. 9.11-9.20 (1977).

47. De Ruyck, J., C. Hirsch and P. Kool, "An Axial Compressor End Wall Boundary Layer Prediction Method," Transactions of ASME, Journal of Engineering for Power, 101, pp. 233-249 (1979).
48. De Ruyck, J. and C. Hirsch, "Investigations of an Axial Compressor End-Wall Boundary Layer Prediction Method," Transactions of ASME, Journal of Engineering for Power, 103, pp. 20-33 (1981).
49. Dring, R. P., "A Momentum-Integral Analysis of the Three-Dimensional Turbine End-Wall Boundary Layer," Transactions of ASME, Journal of Engineering for Power, 93, pp. 386-396 (1971).
50. Dunham, J., "A Review of Cascade Data on Secondary Losses in Turbines," Journal of Mechanical Engineering Science, 12, pp. 48-59 (1970).
51. Dyne, G., "A Streamline Curvature Method for Calculating the Viscous Flow Around Bodies of Revolution," International Symposium on Ship Viscous Resistance, SSPA Goteborg, pp. 6.1-6.22 (1978).
52. East, L.F., "A Prediction of the Law of the Wall in Compressible Three-Dimensional Turbulent Boundary Layers," R.A.E. TR-72178 (1972).
53. East, L.F., "Computation of Three-Dimensional Turbulent Boundary Layers," Aeronautical Research Institute of Sweden (FFA), Technical Note AE-1211 (Sep 1975); also, T.K. Fannelp and P.A. Krogstad, "Three-Dimensional Turbulent Boundary Layers in External Flows: A Report on Euromech 60," Journal of Fluid Mechanics, 71, pp. 815-826 (1975).

54. East, L.F., "A Representation of Second Order Boundary Layer Effects in the Momentum Integral Equations and in Viscous-Inviscid Interaction," R.A.E. TR-81002 (1981).
55. East, L.F. and R.P. Hoxey, "Boundary Layer Effects in an Idealized Wing-Body Junction at Low Speed," R.A.E. TR-68161 (Jul 1968).
56. East, L.F. and R.P. Hoxey, "Low-Speed Three-Dimensional Turbulent Boundary Layer Data, Parts 1 and 2," A.R.C. R&M No. 3653 (Mar 1969).
57. East, L.F., P.D. Smith and P.J. Merryman, "Prediction of the Development of Separated Turbulent Boundary Layers by the Log-Entrainment Method," R.A.E. TR77046 (1977).
58. East, L.F. and W.G. Sawyer, "An Investigation of the Structure of Equilibrium Turbulent Boundary Layers," AGARD-CP-271: Turbulent Boundary Layers, pp. 6.1-6.19 (1980).
59. Elsenaar, A., B. van den Berg and J.P.F. Lindhout, "Three-Dimensional Separation of an Incompressible Turbulent Boundary Layer on an Infinite Swept Wing," AGARD-CP-168: Separation in Flows, pp. 34.1-34.15 (1975).
60. Fernholz, H., "Three-Dimensional Turbulent Boundary Layers: A Report on Euromech 33," Journal of Fluid Mechanics, 58, pp. 177-186 (1973).
61. Firmin, M.C.P., "Calculations of Transonic Flow Over Wing/Body Combinations with an Allowance for Viscous Effects," AGARD-CP-291: Computation of Viscous-Inviscid Interaction, pp. 8.1-8.18 (1980).

62. Formery, M. and J. Delery, "Finite Difference Method for the Inverse Mode Computation of a Three-Dimensional Turbulent Boundary Layer", *La Recherche Aerospatiale* 1981-5, pp. 11-21 (1981)
63. Geller, E.W., "Calculation of Flow in the Tail Region of a Body of Revolution," *Journal of Hydronautics*, 13, pp. 127-129 (1979).
64. Gessner, F.B., "The Origin of Secondary Flow in Turbulent Flow Along a Corner," *Journal of Fluid Mechanics*, 58, pp. 1-25 (1973).
65. Gessner, F.B. and A.F. Emery, "A Reynolds Stress Model for Turbulent Corner Flows--Part 1: Development of the Model; Part 2: Comparison between Theory and Experiment," *Transactions of ASME, Journal of Fluids Engineering*, 98, pp. 261-277 (1976).
66. Green, J.E., "Application of Head's Entrainment Method to the Prediction of Turbulent Boundary Layers and Wakes in Compressible Flow," A.R.C. R&M No. 3788 (1972).
67. Green, J.E., D.J. Weeks and J.W.F. Brooman, "Prediction of Turbulent Boundary Layers and Wakes in Compressible Flow by a Log-Entrainment Method," A.R.C. R&M No. 3791 (1973).
68. Hawthorne, W.R., "The Secondary Flow about Struts and Airfoils," *Journal of Aeronautical Science*, 21, pp. 588-608 (1954).
69. Head, M.R., "Entrainment in the Turbulent Boundary Layer," A.R.C. R&M No. 3152 (1958).

70. Herring, J.R., "Subgrid Scale Modeling—An Introduction and Overview," 1st International Symposium on Turbulent Shear Flows, Pennsylvania State University, pp. 347-352 (1977).
71. Hess, J.L., "Review of Integral-Equation Techniques for Solving Potential Flow Problems with Emphasis on the Surface-Source Method," Computer Methods in Applied Mechanics and Engineering, 5, pp. 145-196 (1975).
72. Hoekstra, M. and H.C. Raven, "Calculation of Viscous-Inviscid Interaction in the Flow Past a Ship Afterbody," 13th Symposium on Naval Hydrodynamics, Tokyo, pp. 585-599 (1980).
73. Hoffman, G.H., "A Modified Displacement-Body Method for Treating the Axisymmetric Strong Interaction Problem," Journal of Ship Research, 24, pp. 114-122 (1980).
74. Horlock, J.H., "Cross Flows in Bounded Three-Dimensional Turbulent Boundary Layers," Journal of Mechanical Engineering Science, 15, pp. 274-284 (1973).
75. Horlock, J.H., J.F. Norbury and J.C. Cooke, "Three-Dimensional Boundary Layers: A Report on Euromech 2," Journal of Fluid Mechanics, 27, pp 369-380 (1967).
76. Horlock, J.H. and H. Marsh, "Flow Models for Turbomachines," Journal of Mechanical Engineering Science, 13, pp. 358-368 (1971).
77. Horlock, J.H. and B. Lakshminarayana, "Secondary Flows: Theory, Experiment and Application in Turbomachinery Aerodynamics," Annual Review of Fluid Mechanics, 5, pp. 247-280 (1973).

78. Horlock, J.H. and H.J. Perkins, "Annulus Wall Boundary Layers in Turbo-machines," AGARD No. 185 (1974).
79. Hornung, H.G. and P.N. Joubert, "The Mean Velocity Profile in Three-Dimensional Turbulent Boundary Layers," *Journal of Fluid Mechanics*, 15, pp. 368-385 (1963).
80. Huang, T.T., N. Santelli, and G. Belt, "Stern Boundary-Layer Flow on Axisymmetric Bodies," 12th Symposium on Naval Hydrodynamics, Washington, DC, pp. 127-147 (5-9 Jun 1979).
81. Humphreys, D.A., "Comparison of Boundary Layer Calculations for a Wing: The May 1978 Stockholm Workshop Test Case," Aeronautical Research Institute of Sweden (FFA), Technical Note AE-1522 (Jan 1979); also, D.A. Humphreys, "Three-Dimensional Wing Boundary Layer Calculated with Eight Different Methods," *AIAA Journal*, 19, pp. 232-234 (1981).
82. Hunt, J.C.R., C.J. Abell, J.A. Peterka and H. Woo, "Kinematical Studies of the Flows Around Free or Surface-Mounted Obstacles: Applying Topology to Flow Visualization," *Journal of Fluid Mechanics*, 86, pp. 179-200 (1978).
83. IUTAM Conference, Berlin (Apr 1982).
84. Jischa, M. and K. Homann, "About an Integral Method for Turbulent Boundary Layers Using the Turbulent Energy Equation," Symposium on Turbulent Shear Flows, Pennsylvania State University, pp. 10.43-10.50 (1977).
85. Johnston, J.P., "On the Three-Dimensional Turbulent Boundary Layer Generalized by Secondary Flow," *Transactions of ASME, Journal of Basic Engineering*, 82, pp. 233-248 (1960).

86. Johnston, J.P., "The Turbulent Boundary Layer at a Plane of Symmetry in a Three-Dimensional Flow," Transactions of ASME, Journal of Basic Engineering, 82, pp. 622-628 (1960).
87. Johnston, J.P., "Measurements in a Three-Dimensional Turbulent Boundary Layer Induced by a Swept, Forward-Facing Step," Journal of Fluid Mechanics, 42, pp. 823-844 (1970).
88. Kader, B.A. and A.M. Yaglom, "Similarity Treatment of Moving-Equilibrium Turbulent Boundary Layers in Adverse Pressure Gradients," Journal of Fluid Mechanics, 89, pp. 305-342 (1978).
89. Katz, J., "A Discrete Vortex Method for the Non-Steady Separated Flow Over an Airfoil," Journal of Fluid Mechanics, 102, pp. 315-328 (1981).
90. Kitchens, C.W., N. Garber, R. Sedney, J.M. Bartos, "Streamwise Vorticity Decay Downstream of a Three-Dimensional Protuberance," ARBRL-TR-02375 (1981).
91. Kline, S.J., "1980-81 AFOSR-HTTM-Stanford Conference on Complex Turbulent Flows: Comparison of Computation and Experiment," Stanford, CA (1982).
92. Kline, S.J., M.V. Morkovin, G. Sovran and D.K. Cockrell, ed., "AFOSR-IFP-Stanford Conference on Computation of Turbulent Boundary Layers," (1968).
93. Kline, S.J., J.M. Ferziger and J.P. Johnston, "Calculation of Turbulent Shear Flows: Status and Ten-Year Outlook," Transactions ASME, Journal of Fluids Engineering, 100, pp. 3-5 (1978).

94. Klinksiek, W.F. and F.J. Pierce, "Simultaneous Lateral Skewing in a Three-Dimensional Turbulent Boundary-Layer Flow," Transactions of ASME, Journal of Basic Engineering, 92, pp. 83-92 (1970).
95. Kool, P., "An Heuristic Approach to the Modelling of Three-Dimensional Turbulent Boundary Layers," ZAMM 59, pp. T277-T278 (1979).
96. Kux, J., "Influence of Wall Curvature on Boundary Layer Development on Ship Hulls," 13th Symposium on Naval Hydrodynamics, Tokyo, pp. 617-629 (1980).
97. Lakshminarayana, B. and J.H. Horlock, "Generalized Expressions for Secondary Vorticity Using Intrinsic Coordinates," Journal of Fluid Mechanics, 59, pp. 97-115 (1973).
98. Landweber, L., "Characteristics of Ship Boundary Layers," 8th Symposium on Naval Hydrodynamics, Washington, DC, pp. 449-472 (1970).
99. Landweber, L. and V.C. Patel, "Ship Boundary Layers," Annual Review of Fluid Mechanics, 11, pp. 173-205 (1979).
100. Langston, L.S., "Crossflows in a Turbine Cascade Passage," Transaction of ASME, Journal of Engineering for Power, 102, pp. 866-874 (1980).
101. Langston, L.S., M.L. Nice and R.M. Hooper, "Three-Dimensional Flow within a Turbine Cascade Passage," Transactions of ASME, Journal of Engineering for Power, 99, pp. 21-28 (1977).
102. Larson, L., ed., "SSPA ITTC Workshop on Ship Boundary Layers 1980," Goteborg, Sweden (1981).

103. Launder, B.E., "Reynolds Stress Closures -- Status and Prospects," AGARD-CP-271: Turbulent Boundary Layers, pp. 13.1-13.13 (1980).
104. Launder, B.E. and D.B. Spalding, "The Numerical Computation of Turbulent Flows," Computer Methods in Applied Mechanics and Engineering, 3, pp. 269-289 (1974).
105. Launder, B.E., C.H. Priddin and B.I. Sharma, "The Calculation of Turbulent Boundary Layers on Spinning and Curved Surfaces," Transactions of ASME, Journal of Fluids Engineering, 99, pp. 231-239; also comments by P. Bradshaw, pp. 435-437 (1977).
106. LeBalleur, J.C., "Technical Evaluation Report of the AGARD Fluid Dynamics Panel Symposium on the Computation of Viscous-Inviscid Interaction," AGARD-CP-291: The Computation of Viscous - Inviscid Interaction, pp. 1-15 (1980).
107. LeBalleur, J.C., "Strong Matching Method for Computing Transonic Viscous Flows Including Wakes and Separations. Lifting Airfoils," La Recherche Aerospatiale, 1981-3, pp. 21-45 (1981).
108. Le Balleur, J.C., R. Peyret and H. Viviand, "Numerical Studies in High Reynolds Number Aerodynamics," Computers and Fluids, 8, pp. 1-30 (1980).
109. Lemmerman, L.A. and V.R. Sonnad, "Three-Dimensional Viscous-Inviscid Coupling Using Surface Transpiration," Journal of Aircraft, 16, pp. 353-358 (1979).

110. Leonard, A., "Review: Vortex Methods for Flow Simulation," Journal of Computational Physics 37, pp. 289-335 (1980).
111. Lewkowicz, A.K., D. Hoadley, J.H. Horlock, and H.J. Perkins, "A Family of Integral Methods for Predicting Turbulent Boundary Layers," AIAA Journal, 8, pp. 44-51 (1970).
112. Lighthill, M.J., "On Displacement Thickness," Journal of Fluid Mechanics, pp. 383-392 (1958).
113. Lighthill, M.J., "Attachment and Separation in Three-Dimensional Flow in Laminar Boundary Layers," L. Rosenhead, ed., Oxford University Press, pp. 46-114 (1963).
114. Lindhout, J.P.F., B. van den Berg and A. Elsenaar, "Comparison of Boundary Layer Calculations for the Root Section of a Wing: The September 1979 Amsterdam Workshop Test Case," NLR Report MP-80028 (1980).
115. Lindhout, J.P.F., G. Moek, E. de Boer and B. van den Berg, "A Method for the Calculation of Three-Dimensional Layers on Practical Wing Configurations," Transactions of ASME, Journal of Fluids Engineering, 103, pp. 104-111 (1981).
116. Lock, R.C., "A Review of Methods for Predicting Viscous Effects on Aerofoils and Wings at Transonic Speeds," AGARD-CP-291: The Computation of Viscous-Inviscid Interaction, pp. 2.1-2.32 (1980).
117. Lock, R.C. and M.C.P. Firmin, "Survey of Techniques for Estimating Viscous Effects in External Aerodynamics," R.A.E. TR-1900 (1981).

118. Louis, J.F., "Rotational Viscous Flow," Proceedings of the 9th International Congress of Applied Mechanics, pp. 306-317 (1956).
119. Lugt, H.J., "Numerical Modeling of Vortex Flows in Ship Hydrodynamics—A Review," The 3rd International Conference on Numerical Ship Hydrodynamics, Paris (1981).
120. McMahon, H., J. Hubbartt and L. Kubendran, "Mean Velocities and Reynolds Stresses in a Juncture Flow," Status Report, Georgia Institute of Technology (Feb 1981).
121. McNally, W.D. and P.M. Sockol, "Computational Methods for Internal Flows with Emphasis on Turbomachinery," Symposium on Computers in Flow Predictions and Fluid Dynamics Experiments, ASME Winter Annual Meeting, Washington, DC (15-20 Nov 1981).
122. Mahgoub, H.E.H. and P. Bradshaw, "Calculation of Turbulent-Inviscid Flow Interactions with Large Normal Pressure Gradients," AIAA Journal, 17, pp. 1025-1029 (1979).
123. Mani, K.K., "Momentum Integral Method at the Beginning of Crossflow Development," AIAA Journal, 20, pp. 556-559 (1982).
124. Markatos, N.C., M.R. Malin and D.G. Tatchell, "Computer Analysis of Three-Dimensional Turbulent Flows Around Ships' Hulls," Proceedings of Institution of Mechanical Engineers, 194, pp. 239-248 (1980).
125. Markatos, N.C. and C.B. Wills, "Prediction of Viscous Flow Around a Fully Submerged Appended Body," 13th Symposium on Naval Hydrodynamics, Tokyo, pp. 631-650 (1980).

126. Marsh, H. and J.H. Horlock, "Wall Boundary Layers in Turbomachines,"
Journal of Mechanical Engineering Science, 14, pp. 411-423 (1972).
127. Mellor, G.L. and D.M. Gibson, "Equilibrium Turbulent Boundary Layers,"
Journal of Fluid Mechanics, 24, pp. 225-253 (1966).
128. Mellor, G.L. and G.M. Wood, "An Axial Compressor End-Wall Boundary Layer
Theory," Transaction of ASME, Journal of Basic Engineering, 93, pp. 300-
316 (1971).
129. Mellor, G.L. and H.J. Herring, "A Survey of the Mean Turbulent Field
Closure Models," AIAA Journal, 11, pp. 590-599 (1973).
130. Melnik, R.E., "Turbulent Interactions on Airfoils at Transonic Speeds—
Recent Development," AGARD-CP-291: The Computation of Viscous-Inviscid
Interactions, pp. 10.1-10.34 (1980).
131. Meroney, R.N. and P. Bradshaw, "Turbulent Boundary-Layer Growth over a
Longitudinally Curved Surface," AIAA Journal, 13, pp. 1448-1453 (1975).
132. Muraoka, K., "Calculation of Thick Boundary Layer and Wake of Ships by a
Partially Parabolic Method," 13th Symposium on Naval Hydrodynamics, Tokyo,
pp. 601-616 (1980).
133. Myring, D.F., "An Integral Prediction Method for Three-Dimensional Tur-
bulent Boundary Layers in Incompressible Flow," R.A.E. TR-70147 (1970).
134. Myring, D.F., "The Profile Drag of Bodies of Revolution in Subsonic
Axisymmetric Flow," R.A.E. TR-72234 (1972).

135. Myring, D.F., "Pressure Rise to Separation in Cylindrically Symmetric Shock Wave-Turbulent Boundary Layer Interaction," AGARD-CP-168: Separation in Flows, pp. 36.1-36A.2 (1975).
136. Nakayama, A., V.C. Patel and L. Landweber, "Flow Interaction Near the Tail of a Body of Revolution. Part 1: Flow Exterior to Boundary Layer and Wakes; Part 2: Iterative Solution for Flow Within and Exterior to Boundary Layer and Wake," Transactions of ASME, Journal of Fluid Engineering, 98, pp. 531-537; 538-549 (1976).
137. Nash, J.F. and V.C. Patel, "Three-Dimensional Turbulent Boundary Layers," SBC Technical Books, Scientific and Business Consultants, Inc. (1972).
138. Nash, J.F. and V.C. Patel, "Advances in Turbulence Boundary Layer Calculation Methodology," 1st International Symposium on Turbulent Shear Flows, Pennsylvania State University, pp. 5.1-5.11 (1977).
139. Nielsen, Jack N., M.J. Hensch and M.F. Dillenius, "The Induced Rolling Moments of Cruciform Wing-Body Combinations as Influenced by Panel-Panel Interference," Nielsen Engineering and Research, Inc. Report (Nov 1974).
140. Odabasi, A.Y., "GEMAK--A Method for Calculating the Flow Around Aft-End of Ships," 13th Symposium on Naval Hydrodynamics, pp. 747-777 (1980).
141. Oguz, E.A., "An Experimental Investigation of the Turbulent Flow in the Junction of a Flat Plate and a Body of Constant Thickness," PhD Thesis, Georgia Institute of Technology (1981).
142. Orszag, S.A. and M. Israeli, "Numerical Simulation of Viscous Incompressible Flows," Annual Review of Fluid Mechanics, 5, pp. 281-318 (1974).

143. Papailiou, K., R. Flot and J. Mathieu, "Secondary Flows in Compressor Bladings," Transactions of ASME, Journal of Engineering for Power, 99, pp. 211-224 (1977).
144. Patankar, S.V. and D.B. Spalding, "A Calculation Procedure for Heat, Mass and Momentum Transfer in Three-Dimensional Parabolic Flows," International Journal of Heat Mass Transfer, 15, pp. 1787-1805 (1972).
145. Patel, V.C., "On the Equations of a Thick Axisymmetric Turbulent Boundary Layer," The University of Iowa IIHR Report No. 143 (1973).
146. Patel, V.C., A. Nakayama and R. Damain, "Measurements in the Thick Axisymmetric Turbulent Boundary Layer Near the Tail of a Body of Revolution," Journal of Fluid Mechanics, 63, pp. 345-362 (1974).
147. Patel, V.C., Y.T. Lee and O. Guven, "Measurements in the Thick Axisymmetric Turbulent Boundary Layer and the Near Wake of a Low-Drag Body of Revolution," 1st International Symposium on Turbulent Shear Flow, Pennsylvania State University, pp. 9.29-9.36 (18-20 Apr 1977).
148. Patel, V.C. and G. Scheuerer: "Calculation of Two-Dimensional Near and Far Wakes", AIAA Journal 20, pp. 900-907 (1982).
149. Patel, V.C. and Y.T. Lee, "Thick Axisymmetric Boundary Layers and Wakes: Experiment and Theory," International Symposium on Ship Viscous Resistance, SSPA, Goteborg, pp. 4.1-4.20 (1978).
150. Patel, V.C. and D.H. Choi, "Calculation of Three-Dimensional Laminar and Turbulent Boundary Layers on Bodies of Revolution at Incidence," 2nd

151. Peake, D.J. and R.D. Galway, "The Three-Dimensional Separation of a Plane Incompressible Laminar Boundary Layer Produced by a Circular Cylinder Mounted Normal to a Flat Plate," National Research Council of Canada Report LR-428 (May 1965).
152. Peake, D.J., R.D. Galway and W.J. Rainbird, "The Three-Dimensional Separation of a Plane Incompressible Laminar Boundary Layer Produced by a Rankine Oval Mounted Normal to a Flat Plate," National Research Council of Canada Report LR-446 (Nov 1965).
153. Peake, D.J. and M. Tobak, "Three Dimensional Interactions and Vortical Flows with Emphasis on High Speeds," AGARD-AG-252 (180).
154. Perkins, H.J., "The Formation of Streamwise Vorticity in Turbulent Flow," Journal of Fluid Mechanics, 44, pp. 721-740 (1970).
155. Perry, A.E. and P.N. Joubert, "A Three-Dimensional Turbulent Boundary Layer," Journal of Fluid Mechanics, 22, pp. 285-304 (1965).
156. PHOENICS Computer Program: "Parabolic, Hyperbolic or Elliptic Integration Code Series", CHAM Ltd, London, UK (1981).
157. Pierce, F.J., "Near-Wall Similarity in a Pressure-Driven Three Dimensional Turbulent Boundary Layer," Report VPI-E-80.32, Virginia Polytechnic Institute and State University (Sep 1980).
158. Prahlad, T.S., "Mean Velocity Profiles in Three-Dimensional Incompressible Turbulent Boundary Layers," AIAA Journal, 11, pp. 359-365 (1973).

159. Pratap, V.S. and D.B. Spalding, "Numerical Computations of the Flow in Curved Ducts," *Aeronautical Quarterly*, 26, pp. 219-228 (1975).
160. Reynolds, W.C., "Computation of Turbulent Flows," *Annual Review of Fluid Mechanics*, 8, pp. 183-208 (1976).
161. Reynolds, W.C. and T. Cebeci, "Calculation of Turbulent Flows," *Topics in Applied Physics*, Vol. 12, Turbulence, Second Edition, P. Bradshaw, ed. (1978).
162. Rotta, J.C., "Grenzschichttheorie Zweiter Ordnung Fur Ebene und Achsen-symmetrische Hyperschallstromung," *Z. Flugwiss*, 15, pp. 329-334 (1967).
163. Rotta, J.C., "A Family of Turbulence Models for Three-Dimensional Boundary Layers," *1st International Symposium on Turbulent Shear Flows*, Pennsylvania State University, pp. 267-278 (1977).
164. Schofield, W.H., "Equilibrium Boundary Layers in Moderate to Strong Adverse Pressure Gradients," *Journal of Fluid Mechanics*, 113, pp. 91-122 (1981).
165. Sedney, R. and C.W. Kitchens, "The Structure of Three Dimensional Separated Flows in Obstacle, Boundary Layer Interactions," *AGARD-CP-168: Flow Separation*, pp. 37.1-37.15 (1975).
166. Sevik, M., "A Discussion on a Paper by J.B. Hadler and Henry M. Cheng, "Analysis of Experimental Wake Data in Way of Propeller Plane of Single and Twin-Screw Ship Models," *Transactions of SNAME*, 73, pp. 386-389 (1965).

167. Shabaka, I.M.M.A. and P. Bradshaw, "Turbulent Flow in an Idealized Wing-Body Junction," PhD. Thesis, University of London (Apr 1979).
168. Shanebrook, J.R. and W.J. Sumner, "Crossflow Profiles for Compressible Turbulent Boundary Layers," Journal of Aircraft, 8, pp. 188-189 (1971).
169. Shanebrook, J.R. and D.E. Hatch, "A Family of Hodograph Models for the Cross Flow Velocity Component of Three-Dimensional Turbulent Boundary Layers," Transactions of ASME, Journal of Basic Engineering, 94, pp. 321-332 (1972).
170. Shanebrook, J.R. and W.J. Sumner, "Entrainment Equation for Three-Dimensional Compressible Turbulent Boundary Layers," AIAA Journal, 10, pp. 693-694 (1972).
171. Shang, J.S., W.L. Hankey and J.S. Pety, "Three-Dimensional Supersonic Interacting Turbulent Flow Along a Corner," AIAA Journal, 17, pp. 706-713 (1978).
172. Shen, S.F., "Finite-Element Methods in Fluid Mechanics," Annual Review of Fluid Mechanics, 9, pp. 421-445 (1979).
173. Simpson, R.L., "A Review of Some Phenomena in Turbulent Flow Separation," Journal of Fluid Engineering, 103, pp. 520-533 (1981).
174. Simpson, R.L., J.H. Strickland and P.W. Barr, "Features of a Separating Turbulent Boundary Layer in the Vicinity of Separation," Journal of Fluid Mechanics, 79, pp. 553-594 (1977).
175. Smith, J.H.B., "A Review of Separation in Steady Three-Dimensional Flow," AGARD-CP-168: Flow Separation, pp. 31.1-31.17 (1975).

176. Smith, P.D., "Calculation Methods for Three Dimensional Turbulent Boundary Layers," A.R.C. R&M No. 3523 (1966).
177. Smith, P.D., "An Integral Prediction Method for Three Dimensional Compressible Turbulent Boundary Layers," A.R.C. R&M No. 3739 (1972).
178. Squire, H.B. and K.G. Winter, "The Secondary Flow in a Cascade of Airfoils in a Nonuniform Stream," Journal of Aeronautical Science, 18, pp. 271-277 (1951).
179. Stanbrook, A., "Experimental Observation of Vortices in Wing-Body Junctions, A.R.C. R&M No. 3114 (1957).
180. Stewartson, K., "Multistructured Boundary Layers on Flat Plates and Related Bodies," Advances in Applied Mechanics, 14, pp. 145-234 (1974).
181. Stock, H.W., "Computation of the Boundary Layer and Separation Lines on Inclined Ellipsoids and of Separated Flows on Infinite Swept Wings," AIAA 13th Fluid and Plasma Dynamics Conference, Snowmass, Colorado (14-16 Jul 1980).
182. Stratford, B.S., "The Prediction of Separation of the Turbulent Boundary Layer," Journal of Fluid Mechanics, 5, pp. 1-16 (1959).
183. Thompson, B.G.J., "A New Two-Parameter Family of Mean Velocity Profiles for Incompressible Turbulent Boundary Layers on Smooth Walls," A.R.C. R&M No. 3463 (Apr 1965).
184. Tobak, M. and D.J. Peake, "Topology of Two-Dimensional and Three-Dimensional Separated Flow," AIAA 12th Fluid and Plasma Dynamics Conference, Williamsburg, VA (23-25 Jul 1979).

185. Townsend, A.A., "The Behavior of a Turbulent Boundary Layer Near Separation," Journal of Fluid Mechanics, 12, pp. 536-554 (1961).
186. Townsend, A.A., "Equilibrium Layers and Wall Turbulance," Journal of Fluid Mechanics, 11, pp. 97-120 (1961).
187. van den Berg, B., "A Three Dimensional Law of the Wall for Turbulent Shear Flows," Journal of Fluid Mechanics, 70, pp. 149-160 (1975).
188. van den Berg, B., A. Elsenaar, J.P.F. Lindhout and P. Wesseling, "Measurements in an Incompressible Three Dimensional Turbulent Boundary Layer, Under Infinite Swept-Wing Conditions and Comparison with Theory," Journal of Fluid Mechanics, 70, pp. 127-148 (1975).
189. Veldman, A.E.P., "The Calculation of Incompressible Boundary Layers with Strong Viscous-Inviscid Interaction," AGARD-CP-291: Computation of Viscous-Inviscid Interaction, pp. 12.1-12.12 (1980).
190. Veldman, A.E.P., "New Quasi-Simultaneous Method to Calculate Interacting Boundary Layers," AIAA Journal, 19, pp. 79-85 (1981).
191. von Kerczek, C.H., "A New Generalized Cross-Flow Momentum Integral Method for Three Dimensional Ship Boundary Layers," Science Applications, Inc. Report SAI-463-82-085-LJ (1982).
192. Wang, K.C., "On the Determination of the Zones of Influence and Dependence for Three-Dimensional Boundary-Layer Equations," Journal of Fluid Mechanics, 43, pp. 397-404 (1971).

193. Wang, H.T. and T.T. Huang, "Calculation of Potential Flow/Boundary Layer Interaction on Axisymmetric Bodies," International Symposium on Ship Viscous Resistance, pp. 47-57 (1978).
194. Webster, W.C., "The Flow About Arbitrary, Three-Dimensional Smooth Bodies," Journal of Ship Research, 19, pp. 206-218 (1975).
195. Wheeler, A.J. and J.P. Johnston, "An Assessment of Three-Dimensional Turbulent Boundary Layer Prediction Methods," Transactions of ASME, Journal of Fluids Engineering, 95, pp. 415-421 (1973).
196. Whitfield, D.L., "Analytical Description of the Complete Turbulent Boundary Layer Velocity Profile," AIAA Journal, 17, pp. 1145-1147 (1979).
197. Whitfield, D.L., T.W. Swafford and J.L. Jacocks, "Calculation of Turbulent Boundary Layers with Separation and Viscous-Inviscid Interaction," AIAA Journal, 19, pp. 1315-1322 (1981).
198. Williams, III, J.C., "Incompressible Boundary Layer Separation," Annual Review of Fluid Mechanics, 9, pp. 113-144 (1977).
199. Zwaaneveld, J., "Comparison of Various Methods for Calculating Profile Drag from Pressure Measurements in the Near Wake at Subcritical Speeds," AGARD-CP-124: Aerodynamic Drag, pp. 10.1-10.A3 (1973).

TABLE A1 -

HIGHLIGHTS OF THE BIBLIOGRAPHY

BIBLOG. NO.	THEORY	EXPERIMENT	NUMERICAL METHODS		TYPE OF PROBLEMS	APPROXIMATIONS OR MODELS	COMMENTS
			DIFFERENTIAL	INTEGRAL			
1.	x		x		3-D Turbulent boundary layers on ship hulls	Two-equation turbulence model	Comparisons indicate that the partially parabolic solution is far superior to the parabolic one
2.	x		x		3-D turbulent boundary layers on ship hulls	Two-equation turbulence model	A partially parabolic system with a two-equation turbulence model is considered in a non-orthogonal coordinate system
3.	x		x		Corner flows		The streamwise vorticity equation is used to avoid the use of transverse momentum equations
4.		x			Laminar horseshoe vortex	Smoke flow visualization	The number and the oscillatory behavior of horseshoe vortices increase as the Reynolds number increases
5.		x			Flow in Strut-wall intersection	Flow visualization and transverse flow measurements	The thickness of the incident boundary layers determines the size of the horseshoe vortex
6.	x		x		3-D compressible Navier-Stokes equations		An alternative and parallel numerical method to the LBI scheme developed by Briley and McDonald (Bibl. 16&17)
7.		x			Flow about circular cylinders mounted on a flat plate	Laminar and turbulent	Shows that the size of the horseshoe vortex can be characterized by the Reynolds number based on the thickness of the incident boundary layer
8.	x				The effects of streamline curvatures		This is an attempt to account for the effects of streamline curvature while still in the frame work of thin boundary layer approximation
9.	x				The effects of streamline curvatures		A more detailed and further exploration of the above paper (Bibl. 8)
10.	x		x		3-D turbulent boundary layer		The rate-equation turbulence model derived for 2-D in bibl. 14 is extended to 3-D flows
11.	x				Review of complex turbulent flows		The importance of an accurate potential flow calculation and the "history" of the flow for strongly "interacting" flows is pointed out.
12.	x				Structure of complex turbulence flows		The concept of the "fairly thin shear layer" was introduced for the prediction of thick boundary layers within the frame work of the thin boundary layer approximation.

BIBLIOG. NO.	THEORY	EXPERIMENT	NUMERICAL METHODS		TYPE OF PROBLEMS	APPROXIMATIONS OR MODELS	COMMENTS
			DIFFERENTIAL	INTEGRAL			
13.	x		x		2-D and 3-D separated flows	Thin boundary layer	Both the prediction of separation and the calculation method in the separated region are discussed
14.	x		x		2-D turbulent boundary layer		The rate-equation (or one-equation) turbulence model is derived. The model performed very well in the 1968 Stanford conference (Bibl. 92)
15.	x	x		x	Turbulent corner flow	Thin boundary layer	Reasonable results are obtained except near the separation region.
16.	x		x		3-D compressible Navier Stokes equations	Parabolic-Hyperbolic system	An alternating-direction implicit (ADI) numerical scheme is developed. The main feature is a narrow-banded matrix which can be solved efficiently.
17.	x		x		3-D compressible Navier Stokes equations	Parabolic-Hyperbolic system	Further development of the above so called "linearized block ADI implicit scheme" (LBI scheme)
18.	x		x		Viscous primary and secondary flows		The streamwise vorticity equation is used to avoid the use of transverse momentum equations
19.	x		x		Horseshoe vortex flow	Low Reynolds number ($R_n = 200, 400$). Thin incidence boundary layer	A first step to solving turbulent horseshoe vortex flows
20.	x				Review of laminar separation		A mathematical treatment
21.	x		x		Viscous flows including separation	Axisymmetric body	The matching takes place in the inviscid region far from the region of strong viscous/inviscid interactions
22.	x				Potential flow		The theory of the PAN-AIR computer code is described
23.	x		x		Separated flows		A new viscous/inviscid interaction method is used to improve the convergent rate of the previous method (Bibl. 24)
24.	x		x		Separated flows both laminar and turbulent		Both the viscous/inviscid interaction and the inverse mode are used.
25.	x		x		Separated flow	2-D and laminar	One of the pioneer works in the calculation of the separated flow by the inverse mode

BIBLOC. NO.	THEORY	EXPERIMENT	NUMERICAL METHODS		TYPE OF PROBLEMS	APPROXIMATIONS OR MODELS	COMMENTS
			DIFFERENTIAL	INTEGRAL			
26.	x		x		"Thick" boundary layer along a slender cylinder of constant radius	Thin boundary layer	That the thin boundary layer approximation is adequate for this type of "thick" boundary layer is demonstrated
27.	x		x		3-D laminar and turbulent boundary layers on ship hulls	Thin boundary layer	The implementation to account for the thick boundary layer by the displacement thickness method is mentioned but not done
28.	x		x		3-D laminar and turbulent boundary layers	Body of revolution at incidence	Calculation of flow reversal in the circumferential direction and the prediction of the separation line are discussed
29.	x		x		Laminar and turbulent leading edge separation	Thin airfoil at incidence	A quasi-rational approach is adopted
30.	x		x		Comparison of turbulence closure models		4 two-equation models are compared
31.	x				Survey of computation aerodynamics development and outlook		Both computer hardwares and numerical techniques are discussed
32.	x				Discrete vortex method	2-D time-dependent Navier-Stokes equations	A pioneer work on the application of the discrete vortex method to boundary layer flows at high Reynolds numbers
33.	x				Discrete vortex method		Among other things, the rate of convergence of the solution is improved. Some discussions to include turbulence are also given
34.	x				Review of discrete vortex methods on boundary layer calculations		The current state-of-the-art is still restricted to flows in simple geometries
35.		x			Structure of 2-D turbulent boundary layers with separation	flat plate at zero incidence	Bradshaws' one-equation turbulence model gave good predictions
36.	x				The law of the wake in 2-D turbulent boundary layers		Based on many experimental data, a 2-D law of the wall-wake was proposed.
37.	x				2-D turbulent boundary layers		A very complete compilation and analysis of available data of 2-D turbulent boundary layers
38.	x				Separation in flows		Both laminar and turbulent 2-D and 3-D are discussed with regard to their general properties

BIBLOC. NO.	THEORY	EXPERIMENT	NUMERICAL METHODS		TYPE OF PROBLEMS	APPROXIMATIONS OR MODELS	COMMENTS
			DIFFERENTIAL	INTEGRAL			
39.	x	x		x	Turbulent boundary layer with a longitudinal surface curvature	Thin boundary layer	The technique developed by Bradshaw to account for surface curvature effects is applied
40.	x			x	Calculation of separated turbulent boundary layers	Thin boundary layer	The nature of separation as mathematical singularity is first discussed followed by a discussion on the inverse method to treat separated flows
41.	x			x	3-D separated turbulent boundary layers	Thin boundary layer	The nature of singularity is discussed by considering the properties of the roots of the characteristics equations
42.	x			x	Mean velocity profiles		Some justifications for the use of the mean velocity profiles obtained in 2-D turbulent boundary layers to 3-D problems are discussed
43.	x			x	3-D turbulent boundary layers over an infinite swept wing	Mager's crossflow profile and Thompson's streamwise velocity profile	An orthogonal curvilinear coordinate system is used
44.	x				2-D separation	Laminar flows	Stratford's prediction method for separation is modified
45.	x		x		Horseshoe vortex flow	Low Reynolds number ($R_n = 100, 500$)	Since the flow is laminar, the horseshoe vortex is small and the non-reversal secondary flow predominates the reversal one
46.		x			Turbulent flow about a teardrop body mounted on a flat plate	Only the leading edge region is considered	A large angle between the velocity gradient vector and the wall shear stress vector (anisotropic shear) is observed
47.	x			x	End-wall boundary layer in turbomachine	Pitch-averaged flow	A new crossflow model was introduced but crossover type was not considered
48.	x			x	End-wall boundary layer in turbomachine	Pitch-averaged flow	Improvement of the method described in Bibl. 47 such that flow reversal in the streamwise direction is prohibited
49.	x			x	End-Wall boundary layer in turbomachine	No crossover crossflow	Both Mager's and Johnston's crossflow model are considered
50.	x	x			Review of secondary losses in turbines		The secondary losses include the losses due to the annulus wall boundary layers and their interactions with blade rows
51.	x		x	x	Thick turbulent boundary layers	Body of revolution	The normal pressure gradient is set equal to the centrifugal force due to the longitudinal streamline curvature

BIBLOC. NO.	THEORY	EXPERIMENT	NUMERICAL METHODS		TYPE OF PROBLEMS	APPROXIMATIONS OR MODELS	COMMENTS
			DIFFERENTIAL	INTEGRAL			
52.	x	x			3-D turbulent boundary layer	Semi-analytic solution	Bradshaw's one-equation turbulence model was improved for the prediction of flow with anisotropic shear stress
53.	x		6	3	Comparison of numerical methods on 3-D turbulent boundary layers	7 test cases	The momentum integral method by P. D. Smith did well
54.	x			x	Thick boundary layer	2-D	A formulation of the second-order boundary layer equations with a new, strong viscous/inviscid interaction is given
55.		x			Turbulent flow about a teardrop body mounted on a flat plate	Only the first quadrant of the leading edge region is considered	Both Mager's and Coles' models do not fit the data; Johnston's model has a better fit
56.		x			Turbulent flow about a teardrop body mounted on a flat plate	Only the first quadrant of the leading edge region is considered	The flow in the separated region is characterized by a single concentration of vorticity (horseshoe vortex)
57.	x			x	2-D separated turbulent boundary layers	Lag-entrainment method	An exploratory work on the use of momentum integral methods to calculate separated flows
58.	x	x			Structure of equilibrium turbulent boundary layers	2-D	Seven turbulent boundary layers ranging from mildly favorable to severe adverse pressure gradients were shown to be good approximations to 2-D equilibrium flows
59.	x	x	x		3-D turbulent boundary layer approaching separation	Thin boundary layer	Bradshaw's one-equation turbulence model is used but it fails to predict separation
60.	x	x	x	x	Review of experiments and predictions of 3-D turbulent boundary layers	..	No computational method of the flow in the wing-body junction is presented in the colloquium
61.	x			x	3-D boundary layer and wake over a wing/body combination	Lag-entrainment equation	The horseshoe vortex generated in the wing/body junction is suppressed
62.	x		x		Turbulent horseshoe vortex flow	Thin boundary layer	The inverse mode of computation is used to march across the separation line
63.	x		x		Thick turbulent boundary layer	Body of revolution	The tail region is calculated by the vorticity equation

BIBLOG. NO.	THEORY	EXPERIMENT	NUMERICAL METHODS		TYPE OF PROBLEMS	APPROXIMATIONS OR MODELS	COMMENTS
			DIFFERENTIAL	INTEGRAL			
64.	x	x			Turbulent corner flow	Based on energy and vorticity consideration	The origin of the secondary flow in the corners is due to the transverse gradients of the Reynolds shear stress
65.	x		x		Turbulent corner flow	Thin boundary layer approximation with an algebraic Reynolds stress model	Predicted Reynolds stress distributions were compared with experimental data
66.	x			x	Turbulent boundary layer and wake	2-D	The main features are the treatment of the wake and the formulas for skin friction and shape factor are derived from the zero pressure gradient case
67.	x			x	Turbulent boundary layer and wake	2-D	Derives the lag-entrainment equation which is the integral-method version of Bradshaw's one-equation turbulence model
68.	x	x			Secondary flow about struts and airfoils	Inviscid theory	Comparisons between theory and experiment are made
69.	x			x	Turbulent boundary layer	2-D	The use of the entrainment equation as an auxiliary equation is introduced for the first time
70.	x				Review of subgrid scale modeling		Prediction methods based on subgrid scale modeling are important for flows where the range of length scales is very wide
71.	x				Potential flow	Panel method	Emphasis is on the quadrilateral panel method
72.	x		x		Viscous flows over ship sterns	Thin boundary layer	The viscous-inviscid interaction approach is strongly criticized due to a non-local reaction of the boundary layer
73.	x		x	x	Thick turbulent boundary layers	Body of revolution	A modified displacement thickness method is used to account for the normal pressure gradient
74.	x				Crossflow models in turbomachine		Available crossflow models are reviewed and a new model is proposed
75.	x	x	x	x	A review of 3-D turbulent boundary layers		The prediction of separation, corner flows and secondary flows are discussed

BIBLIOG. NO.	THEORY	EXPERIMENT	NUMERICAL METHODS		TYPE OF PROBLEMS	APPROXIMATIONS OR MODELS	COMMENTS
			DIFFERENTIAL	INTEGRAL			
76.	x				Flows in turbomachines	Inviscid theory	The concept of averaging the flow across the pitch (i.e. the passage-averaged flow) is introduced
77.	x	x			Review of secondary flows		Both theory and experiment are discussed with an emphasis on turbomachine applications
78.	x			x	Review of flows in turbomachines		The application of momentum integral methods is emphasized
79.		x			Turbulent flow about a cylinder mounted on a flat plate	Only the first quadrant in the leading edge of the cylinder is considered	Johnston's mean velocity profile model has a better correlation than that of Coles' model
80.		x			Thick turbulent boundary layers	Body of revolution	Pressure distributions, mean velocity profiles and Reynolds shear stresses are measured. A parallel work to Bibl. 146 and 148
81.	x		5	3	Comparison of numerical methods on a 3-D wing turbulent boundary layer	1 test case	Despite the relative simplicity of the test case, the over-all prediction is not very good
82.	x	x			3-D separation of flows		Application of topology to flow visualization of the flows around free or surface-mounted obstacles
83.	x				Comparison of numerical methods	3 test cases	The flow around a cylinder mounted on a flat plate is one of the test cases
84.	x			x	2-D turbulent boundary layer	Coles' model	Instead of the entrainment equation, the energy equation is used and is shown to be adequate even for non-equilibrium turbulent boundary layers
85.		x			Secondary flow of 3-D turbulent boundary layers		The Johnston's triangular (mean velocity profile) model was born
86.	x			x	3-D turbulent boundary layer with a plane of symmetry	Johnston's triangular model	A good agreement between calculation and measurement is obtained in the non-separated region
87.		x		*	3-D turbulent boundary layer induced by a step		The angle between the mean velocity gradient vector and the shear stress vector is significant even close to the wall. Thus, the eddy-viscosity model is not adequate for the flow considered

BIBLOG. NO.	THEORY	EXPERIMENT	NUMERICAL METHODS		TYPE OF PROBLEMS	APPROXIMATIONS OR MODELS	COMMENTS
			DIFFERENTIAL	INTEGRAL			
88.	x				Turbulent boundary layers	2-D	A general family of the velocity profiles of 2-D moving-equilibrium turbulent boundary layer was derived
89.	x				Discrete vortex method	2-D	The method is used to calculate the unsteady, separated flow over a 2-D airfoil
90.	x	x			Decay of streamwise vorticity		The streamwise vorticity is found to persist more than 100 protuberance diameters downstream both in laminar and turbulent boundary layers
91.	x		x	x	Comparison of numerical methods on complex turbulent flows	66 test cases	The emphasis was on 2-D and 3-D complex turbulent flows. Integral methods continue to perform adequately.
92.	x		9	20	Comparison of numerical methods on mainly 2-D turbulent boundary layers	33 test cases	No distinct superiority of finite differential methods over integral methods were observed
93.	x				Turbulent shear flows		The current status of prediction methods and ten-year outlook are discussed (in 1978)
94.		x			Turbulent boundary layer flow in a S-shaped channel	Internal flows	No mean velocity profile models are adequate for the resulting crossover type of crossflow
95.	x				Modeling of crossflows		Models of mean velocity profiles include crossover crossflows are proposed
96.	x				Ship boundary layer		A general discussion on the effect of surface curvature upon the calculation of turbulent boundary layers of ship hulls
97.	x				Secondary flows		The governing equations of secondary flows are derived in a rotating coordinate system
98.	x				Review of the characteristics of ship boundary layers	Surface ships	The use of integral methods to ship boundary layers is criticized
99.	x		x	x	Review of numerical methods on ship boundary layers	Surface ships	The use of integral methods to ship boundary layers is criticized

BIBLIOG. NO.	THEORY	EXPERIMENT	NUMERICAL METHODS		TYPE OF PROBLEMS	APPROXIMATIONS OR MODELS	COMMENTS
			DIFFERENTIAL	INTEGRAL			
100.	x				Modeling of the mean velocity profile	Based on the data obtained by Langton et al (Bibl. 101)	A model of crossflow including the crossover type is proposed
101.		x			Turbulent flow within a turbine cascade passage	3-D	In addition to flow visualization, both static pressure and mean velocity are measured
102.	x		7	10	Comparison of numerical methods on 3-D ship boundary layer	2 test cases	Both integral and differential methods have difficulties in the stern region where the turbulent boundary layer is thick
103.	x				Review of turbulence closure models		The emphasis is on two-equation or stress-equation models
104.	x		x		Turbulent flows		The reasons for choosing the K-E (two-equation) turbulence model are carefully explained
105.	x		x		Turbulent boundary layers on spinning and curved surfaces		The effects of surface curvatures are investigated in view of modifying the turbulence model
106.	x				Survey of numerical methods on viscous flows at high Reynolds numbers		The state-of-the-art is examined
107.	x			x	Turbulent boundary layers and wakes including separation	2-D	A new concept of viscous/inviscid interaction and matching is proposed. In this method, both viscous and inviscid flows are calculated simultaneously
108.	x		x	x	Viscous flows	High Reynolds numbers	Numerical methods of both finite differential and momentum integral methods are discussed
109.	x			x	Boundary layer on 3-D wing	No crossflow	The surface transpiration method is found to be equivalent to the displacement surface method in adding viscous corrections
110.	x				Review of vortex methods	2-D and 3-D,	Vortex methods are potentially powerful methods to predict high-Reynolds number flows particularly when separation occurs

BIBLIOG. NO.	THEORY	EXPERIMENT	NUMERICAL METHODS		TYPE OF PROBLEMS	APPROXIMATIONS OR MODELS	COMMENTS
			DIFFERENTIAL	INTEGRAL			
111.	x			x	Turbulent boundary layers	2-D	Comparison of the use of the entrainment energy and moment of momentum equation as an auxiliary equation
112.	x				Displacement thickness	2-D and 3-D	The equivalence of the displacement surface method and the surface transpiration method is illustrated
113.	x				Separation in flows		A good review of the fundamental structure and definition of 3-D separation
114.	x		5	4	Comparison of numerical methods	Root section of a 3-D wing	Momentum integral methods gave more consistent results
115.	x		x		3-D boundary layers on wings	Simple eddy-viscosity turbulence model	Despite the anisotropic nature of the turbulent flow, the simple eddy-viscosity model gives reasonable results
116.	x				Review of numerical methods on boundary layers and wakes of airfoils	Mostly 2-D	Integral methods are emphasized
117.	x				Review of numerical methods used in external aerodynamics	2-D and 3-D	New developments in integral methods are emphasized
118.	x				Viscous secondary flow	Secondary flow is considered as a small perturbation to a 3-D flow	The inclusion of the diffusion of vorticity improves the agreement with the data
119.	x				Review of the numerical modeling of vortex flows		The application to ship hydrodynamics is emphasized
120.		x			Review of the numerical modeling of vortex flows	A symmetric "wing" mounted on a flat plate	Two mean velocity components and three Reynolds shear stress components are measured in the wing/body junction
121.	x		x		Review of computation methods used in turbomachine		A thorough review of various finite differential methods
122.	x		x		Thick boundary layer	2-D	The normal pressure gradient is calculated by an iterative scheme without actually solving the elliptic system of equations

BIBLIOG. NO.	THEORY	EXPERIMENT	NUMERICAL METHODS		TYPE OF PROBLEMS	APPROXIMATIONS OR MODELS	COMMENTS
			DIFFERENTIAL	INTEGRAL			
123.	x			x	3-D laminar boundary layer	Moment of momentum equation	A method for stable transition from 2-D computation to 3-D computation is discussed
124.	x		x		3-D turbulent boundary layers on ship hulls	two-equation model turbulence	A further exposition of Spalding's partially parabolic calculation procedure
125.	x		x		Flow around an appended submerged body	two-equation turbulence model	A simplified version of the 3-D partially parabolic scheme is used. The prediction of the horseshoe vortex is not attempted
126.	x			x	Flows in turbomachines	passage-averaged flow	The governing equations for wall boundary layers in turbomachines are derived
127.	x				Equilibrium turbulent boundary layers	2-D	The emphasis is on the velocity defect profiles (i.e. outer region of the boundary layer)
128.	x			x	End-wall boundary layer theory in turbomachines	3-D	Some approximate profiles of the streamwise and the crossflow velocity are assumed
129.	x				Review of turbulence closure models		Review includes one-equation, two-equation and stress-equation models
130.	x				Review of numerical methods on boundary layers and wakes of airfoils	2-D	Both weak and strong viscous-inviscid interactions are discussed. The asymptotic expansion method is emphasized
131.		x			Turbulent boundary layer over a longitudinally curved surface		A data base for the flow over concave and convex surfaces is established. The comparison with calculations based on Bradshaw's technique (Bibl. 8 and 9) gives good agreement
132.	x		x		Thick boundary layer and wake	Partially parabolic and two-equation turbulence model	The superiority of the two-equation turbulence model is claimed
133.	x			x	3-D turbulent boundary layer	Non-orthogonal coordinate system and entrainment equation	Discussions of the characteristics and the numerical procedures of the governing equations are given
134.	x			x	Boundary layer and wake of a body of revolution	Coles' model and entrainment equation	The displacement surface method is used to account for the normal pressure gradient in the thick turbulent boundary layer

BIBLOC. NO.	THEORY	EXPERIMENT	NUMERICAL METHODS		TYPE OF PROBLEMS	APPROXIMATIONS OR MODELS	COMMENTS
			DIFFERENTIAL	INTEGRAL			
135.	x			x	3-D turbulent boundary layer approaching separation	Hager's crossflow model and entrainment equation	Interest centers on the prediction of the pressure rise to separation
136.	x			x	Thick turbulent boundary layer and near wake	A linear crossflow profile assumed	Additional terms due to surface curvature effects are included
137.	x		x	x	Review of 3-D turbulent boundary layer		Detailed derivations of the governing equations are given. Emphasis are on momentum integral methods
138.	x		x	x	Review of advances in 3-D turbulent boundary layer		Both finite differential and momentum integral methods are surveyed
139.	x				Missiles aerodynamics	Inviscid rotational flow	The forces on wing/body combinations at angles of attack
140.	x		x	x	Ship-stern boundary layer	Surface ships	Contains an extensive literature survey
141.		x			Turbulent flow in a wing/body junction	A symmetric "wing" mounted on a flat plate	Pressure, mean velocity components and RMS velocity fluctuation are measured at two boundary layer thicknesses
142.	x				Review of spectral methods		The use of spectral methods for the prediction of viscous flow is still in the research stage
143.	x	x		x	Review of flows in turbomachines	3-D	Various experimental data, theories and computation methods of end-wall boundary layers in turbomachines are discussed
144.	x		x		Calculation procedure for parabolic flows	3-D	The pressure in the streamwise momentum equation is decoupled by averaging over the cross-section. Then a calculation procedure with forward marching method is established.
145.	x		x	x	Thick turbulent boundary layer	Body of revolution	Equations adequate for thick turbulent boundary layers are derived, but the effect of the longitudinal curvature is not included.
146.		x			Thick turbulent boundary layer	Modified spheroid	Pressure distributions, mean velocity profiles and Reynolds shear stresses are measured
147.		x			Thick turbulent boundary layer and near wake	Low-drag body of revolution	Pressure distributions, mean velocity profiles and Reynolds shear stresses are measured

BIBLOC. NO.	THEORY	EXPERIMENT	NUMERICAL METHODS		TYPE OF PROBLEMS	APPROXIMATIONS OR MODELS	COMMENTS
			DIFFERENTIAL	INTEGRAL			
148.	x	x	x		Wear and far wake	2-D	The model is shown to give good results in near wakes, but, does not give correct results in far wakes.
149.	x	x	x	x	Thick turbulent boundary layer and wake	Body of revolution	The calculations by differential and integral methods are compared with the measurements. No significant difference in accuracy between the two methods is found.
150.	x		x		3-D laminar and turbulent boundary layers	Body of revolution at incidence	The need for a more adequate strong viscous/inviscid interaction scheme is indicated for this type of flow.
151.	x	x		x	Laminar flows about circular cylinders mounted on a flat plate	Small crossflow	Agreement between calculation and measurement is in general good before separation. The inaccuracy is blamed on inadequate potential flow calculation.
152.	x	x		x	Rankine ovals mounted on a flat plate	Small cross flow	Same comments as in Bibl. 151. The separated regions are smaller when the boundary layers are turbulent.
153.	x	x			Review of 3-D interactions and vortical flows	Mostly inviscid	The emphasis is on high-speed aircraft. An extensive list of references is provided.
154.	x	x			Turbulent corner flow		The mean streamwise vorticity is shown to arise from mean flow skewing and the inhomogeneity of anisotropic wall turbulence.
155.	x				Modeling of the mean velocity profile	Based on the data of Hornung & Jonbert	The inner and outer regions of the 3-D turbulent boundary layer are considered.
156.	x		x		General purpose viscous flow codes		A computer code for solving parabolic, hyperbolic and elliptic type of the governing equations.
157.		x			Turbulent flow in the leading edge region of a teardrop body on a flat plate	Only the first quadrant of the leading edge region outside of the separation line are considered	Mean velocity component, static pressure and skin friction are measured; no adequate 3-D similarity law is found to fit the data.
158.	x	x			Mean velocity profile of the flow about a teardrop body mounted on a flat plate		Data further downstream of those obtained in Bibl. 56 and 79 are measured.

BIBLOC. NO.	THEORY	EXPERIMENT	NUMERICAL METHODS		TYPE OF PROBLEMS	APPROXIMATIONS OR MODELS	COMMENTS
			DIFFERENTIAL	INTEGRAL			
159.	x		x		Flow in curved ducts		The partially parabolic system with the K-E (two-equation) turbulence model is applied to compute duct flows
160.	x				Review of turbulence closure models		The review includes models of zero-equation, one-equation, two-equation stress-equation and large eddy simulation
161.	x				Review of both turbulence closure models and numerical methods		The current status of momentum integral methods is also discussed
162.	x			x	Thick boundary layers	2-D	The second-order boundary layer equations are derived to account for effects due to surface curvatures
163.	x				Turbulence closure models for 3-D boundary layers		Attempts are made to account for anisotropic shear stress
164.	x				Structure of turbulent boundary layers	2-D	An extension of the previous analysis Bibl. 156
165.		x			Separated flows due to protuberances	Flow visualization	Multiple vortices are observed. A some what weak correlation between the separation distance and the protuberance is also observed
166.		x			Wakes of tail-fin/body intersections	Body of revolution	Demonstrates the importance of the interference effects of tail-fin/body intersections
167.		x			Turbulent flow in a wing/body junction	A symmetric "wing" mounted on a flat plate	Static pressure, skin friction, mean velocity components and Reynolds shear stresses are measured along the junction
168.	x				Modeling of crossflow	Based on a polynomial representation	The (π_i, q_i) family of crossflow models are proposed. The models include cross-over type crossflow
169.	x			x	Crossflows in 3-D turbulent boundary layers	Thin boundary layer approximation with the (π_i, q_i) family of crossflow models	Comparison is made with the data of skewed turbulent boundary layers
170.	x			x	3-D turbulent boundary layer	Entrainment equation	Extension of Head's entrainment equation for incompressible flow to compressible flow
171.	x		x		Turbulent corner flow	3-D	A two layer eddy-viscosity turbulence model is used

BIBLIOG. NO.	THEORY	EXPERIMENT	NUMERICAL METHODS		TYPE OF PROBLEMS	APPROXIMATIONS OR MODELS	COMMENTS
			DIFFERENTIAL	INTEGRAL			
172.	x				Review of finite-element methods in fluid mechanics		Only fundamental aspects are discussed
173.	x	x			Review of separation phenomena in turbulent flow		The experimental aspect of separation was emphasized, but some descriptions of modelings and prediction methods are also discussed
174.		x			Structure of separating 2-D turbulent boundary layer	Airfoil-type pressure distribution	The main features of the flow in the vicinity of separation are discussed
175.	x				Review of separation in steady, flows	3-D	Emphasis is on modeling and structure of separation
176.	x			x	3-D turbulent boundary layer on an infinite yawed wing	Entrainment equation	The results obtained by using different skin friction formulas and mean velocity profiles etc are compared. The polynomial type of velocity profiles is found to be unsatisfactory
177.	x			x	3-D turbulent boundary layers	Non-orthogonal coordinate system and entrainment equation	Johnston's crossflow profile is found more adequate than Mager's profile in the problems where the Reynolds number is high
178.	x				Secondary flow in a cascade passage	Inviscid theory	Pioneer work in secondary flow
179.		x			Rectangular-wing/body and delta-wing/body combinations	Oil-flow visualization and surface pressure distributions	The effects of flow incidence and the Reynolds number on the strength and the position of the vortices are also investigated
180.	x				Review of the structure of laminar boundary layers		The triple-deck structure of laminar boundary layer is described
181.	x			x	Prediction of separation lines and calculation of separated flows	Inclined ellipsoids and infinite swept-wings	A new crossflow profile derived from the profile of a flat plate is used
182.	x				Prediction of separation in turbulent boundary layers	2-D	One of the best engineering prediction methods for separation in 2-D turbulent boundary layers
183.	x				Turbulent boundary layers	2-D	A new family of mean velocity profiles is proposed. The skin friction obtained from this family is an improvement over that by Ludwig and Tillmann

BIBLIOG. NO.	THEORY	EXPERIMENT	NUMERICAL METHODS		TYPE OF PROBLEMS	APPROXIMATIONS OR MODELS	COMMENTS
			DIFFERENTIAL	INTEGRAL			
184.	x	x			Separations in flows	2-D and 3-D	The topology of separations occurring in aircrafts is discussed
185.	x				Turbulent boundary layer near separation		The behavior of the turbulent boundary layer is discussed; a fundamental paper
186.	x				Equilibrium turbulent boundary layers		The type and the structure of equilibrium turbulent boundary layers are discussed; a fundamental paper
187.	x				Law of the wall	3-D	The 3-D law of the wall was derived with the effects of both pressure gradients and inertial forces accounted for
188.	x	x	x		3-D turbulent boundary layer over an infinite swept-wing	No surface curvature effect	Despite the anisotropy of the shear stress, computation based on Bradshaw's model give good results
189.	x		x		Separated flows	Laminar flows	The quasi-simultaneous method is developed as an alternative of the direct and the inverse mode
190.	x				Separated flows	Laminar flows	The quasi-simultaneous method is developed as an alternative of the direct and the inverse mode
191.	x			x	Turbulent boundary layer in a ship hull	Thin boundary layer	A new crossflow model is used
192.	x				Classification of 3-D boundary layer equations		The zones of influence and dependence are discussed in terms of subcharacteristics
193.	x		x		Flow around axisymmetric bodies	Thin boundary layer	The normal pressure gradient is accounted for by the displacement thickness method
194.	x				Potential flow	Panel method	The triangular panel method with a linear source strength is developed
195.	x		x		Assessment of 3-D turbulent boundary layer prediction methods	10 test cases	The test cases include East and Hoxey's wing-body junction flow. Bradshaw's rate-equation (or one-equation) turbulence model is recommended
196.	x			.	Modeling of mean velocity profile	2-D flow	An analytic expression of the mean velocity is proposed and a comparison with the measurement is also made
197.	x			x	Turbulent boundary layers with separation	Mean-flow kinetic energy integral (instead of entrainment equation)	A new multi-layer velocity profile is used

BIBLIOG. NO.	THEORY	EXPERIMENT	NUMERICAL METHODS		TYPE OF PROBLEMS	APPROXIMATIONS OR MODELS	COMMENTS
			DIFFERENTIAL	INTEGRAL			
198	x				Review of laminar separation		Review includes 2-D, 3-D and unsteady separation. This review is an update of the review by Brown and Stewartson (Bibl. 20)
199	x			x	Thick boundary layers	2-D	The main interest of this paper is the formulation of the momentum integral equation to account for a normal pressure gradient given in the Appendix

REFERENCES

1. Patel, V.C., A. Nakayama and R. Damain, "Measurements in the Thick Axisymmetric Turbulent Boundary Layer Near the Tail of a Body of Revolution," *Journal of Fluid Mechanics*, 63, pp. 345-362 (1974).
2. Patel, V.C., Y.T. Lee and O. Guven, "Measurements in the Thick Axisymmetric Turbulent Boundary Layer and the Near Wake of a Low-Drag Body of Revolution," 1st International Symposium on Turbulent Shear Flow, Pennsylvania State University, pp. 9.29-9.36 (18-20 Apr 1977).
3. Huang, T.T., N. Santelli, and G. Belt, "Stern Boundary-Layer Flow on Axisymmetric Bodies," 12th Symposium on Naval Hydrodynamics, Washington, D.C., pp. 127-147 (5-9 Jun 1979).
4. Cebeci, T, "Laminar and Turbulent Incompressible Boundary Layers on Slender Bodies of Revolution in Axial Flow," *Transactions of ASME, Series D, Journal of Basic Engineering*, 92, pp. 545-550 (1970).
5. Barber, T. J., "An Investigation of Strut-Wall Intersection Losses," *Journal of Aircraft*, 15, pp. 576-681 (1978).
6. Sevik, M., "A Discussion on a Paper by J.B. Hadler and Henry M. Cheng, "Analysis of Experimental Wake Data in Way of Propeller Plane of Single and Twin-Screw Ship Models," *Transactions of SNAME*, 73, pp. 386-389 (1965).
7. Baker, C.J., "The Laminar Horseshoe Vortex," *Journal of Fluid Mechanics*, 95, pp. 347-367 (1979).
8. Peake, D.J., R.D. Galway and W.J. Rainbird, "The Three-Dimensional Separation of a Plane Incompressible Laminar Boundary Layer Produced by a Rankine Oval Mounted Normal to a Flat Plate," *National Research Council of Canada Report LR-446* (Nov 1965).

9. Stanbrook, A., "Experimental Observation of Vortices in Wing-Body Junctions, A.R.C. R&M No. 3114 (1957).
10. East, L.F. and R.P. Hoxey, "Low-Speed Three-Dimensional Turbulent Boundary Layer Data, Parts 1 and 2," A.R.C. R&M No. 3653 (Mar 1969).
11. Klinksieck, W.F. and F.J. Pierce, "Simultaneous Lateral Skewing in a Three-Dimensional Turbulent Boundary-Layer Flow," Transactions of ASME, Journal of Basic Engineering, 92, pp. 83-92 (1970).
12. Prahlad, T.S., "Mean Velocity Profiles in Three-Dimensional Incompressible Turbulent Boundary Layers," AIAA Journal, 11, pp. 359-365 (1973).
13. Shabaka, I.M.M.A. and P. Bradshaw, "Turbulent Flow in an Idealized Wing-Body Junction," PhD. Thesis, University of London (Apr 1979).
14. Cooke, J.C. and G.G. Brebner, "The Nature of Separation and Its Prevention by Geometric Design in a Wholly Subsonic Flow," in "Boundary Layer and Flow Control," G.V. Lachmann ed., Vol. 1, pp. 144-185 (1961).
15. Lighthill, M.J., "Attachment and Separation in Three-Dimensional Flow in Laminar Boundary Layers," L. Rosenhead, ed., Oxford University Press, pp. 46-114 (1963).
16. Peake, D.J. and M. Tobak, "Three Dimensional Interactions and Vortical Flows with Emphasis on High Speeds," AGARD-AG-252 (1980).
17. Tobak, M. and D.J. Peake, "Topology of Two-Dimensional and Three-Dimensional Separated Flow," AIAA 12th Fluid and Plasma Dynamics Conference, Williamsburg, VA (23-25 Jul 1979).
18. Dechow, R. and K.O. Felsch, "Measurement of the Mean Velocity and of the Reynolds Stress Tensor in a Three Dimensional Turbulent Boundary Layer Induced by a Cylinder Standing on a Flat Wall," Symposium on Turbulent Shear Flow, Pennsylvania State University, pp. 9.11-9.20 (1977).

19. East, L.F., "A Prediction of the Law of the Wall in Compressible Three-Dimensional Turbulent Boundary Layers," R.A.E. TR-72178 (1972).
20. Johnston, J.P., "Measurements in a Three-Dimensional Turbulent Boundary Layer Induced by a Swept, Forward-Facing Step," Journal of Fluid Mechanics, 42, pp. 823-844 (1970).
21. Belik, L., "The Secondary Flow About Circular Cylinders Mounted Normal to a Flat Plate," Aeron Quart. 24, pp. 47-54 (1973).
22. Le Balleur, J.C., "Technical Evaluation Report of the AGARD Fluid Dynamics Panel Symposium on the Computation of Viscous-Inviscid Interaction," AGARD-CP-291: The Computation of Viscous - Inviscid Interaction, pp. 1-15 (1980).
23. Kline, S.J., J.M. Ferziger and J.P. Johnston, "Calculation of Turbulent Shear Flows: Status and Ten-Year Outlook," Transactions ASME, Journal of Fluids Engineering, 100, pp. 3-5 (1978).
24. Chapman, D.R., "Computational Aerodynamics Development and Outlook", Dryden Lecture, AIAA Journal 17, pp. 1293-1313 (1979).
25. Orszag, S.A. and M. Israeli, "Numerical Simulation of Viscous Incompressible Flows," Annual Review of Fluid Mechanics, 5, pp. 281-318 (1974).
26. Herring, J.R., "Subgrid Scale Modeling-An Introduction and Overview," 1st International Symposium on Turbulent Shear Flows, Pennsylvania State University, pp. 347-352 (1977).
27. Chorin, A.J., "Vortex Models and Boundary Layer Instability," SIAM Journal of Scientific Statistics and Computations, 1, pp. 1-21 (1980).
28. Leonard, A., "Review: Vortex Methods for Flow Simulation," Journal of Computational Physics 37, pp. 289-335 (1980).

AD-A125 792

NUMERICAL WAKE PREDICTION METHODS FOR SUBMERGED
APPENDED BODIES A LITERAT..(U) DAVID W TAYLOR NAVAL
SHIP RESEARCH AND DEVELOPMENT CENTER BET.. C SUNG
FEB 83 DTNSRDC/SPD-1057-01

2/2

UNCLASSIFIED

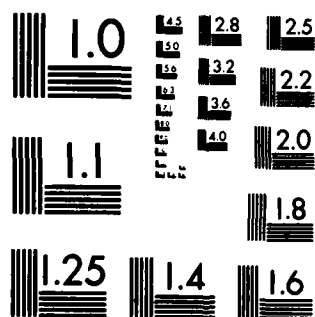
F/G 20/4

NL



END
DATE
FILMED
4 83
DTIC

M-2



MICROCOPY RESOLUTION TEST CHART
NATIONAL BUREAU OF STANDARDS-1963-A

29. Shen, S.F., "Finite-Element Methods in Fluid Mechanics," Annual Review of Fluid Mechanics, 9, pp. 421-445 (1979).
30. Bradshaw, P., D.H. Ferriss, and N.P. Atwell, "Calculation of Boundary-Layer Development Using the Turbulent Energy Equation," Journal of Fluid Mechanics, 28, pp. 593-616 (1967).
31. Patankar, S.V. and D.B. Spalding, "A Calculation Procedure for Heat, Mass and Momentum Transfer in Three-Dimensional Parabolic Flows," International Journal of Heat Mass Transfer, 15, pp. 1787-1805 (1972).
32. Pratap, V.S. and D.B. Spalding, "Numerical Computations of the Flow in Curved Ducts," Aeronautical Quarterly, 26, pp. 219-228 (1975).
33. PHOENICS Computer Program: "Parabolic, Hyperbolic or Elliptic Integration Code Series", CHAM Ltd., London, UK
34. Wang, K.C., "On the Determination of the Zones of Influence and Dependence for Three-Dimensional Boundary-Layer Equations," Journal of Fluid Mechanics, 48, pp. 397-404 (1971).
35. Abdelmeguid, A.A., N.C. Markatos, K. Muraoka, and D.B. Spalding, "A Comparison between the Parabolic and Partially-Parabolic Solution Procedures for Three-Dimensional Turbulent Flows Around Ships' Hulls," Applied Mathematics Modeling 3, pp. 249-258 (1979).
36. Reynolds, W.C., "Computation of Turbulent Flows," Annual Review of Fluid Mechanics, 8, pp. 183-208 (1976).
37. Reynolds, W.C. and T. Cebeci, "Calculation of Turbulent Flows," Topics in Applied Physics, Vol. 12, Turbulence, Second Edition, P. Bradshaw, ed. (1978).
38. Kline, S.J., M.V. Morkovin, G. Sovran and D.K. Cockrell, ed., "AFOSR-IFP-Stanford Conference on Computation of Turbulent Boundary Layers," (1968).

39. Chambers, T.L. and D.C. Wilcox, "Critical Examination of Two-Equation Turbulence Closure Models for Boundary Layers," AIAA Journal, 15, pp. 821-828 (1977).
40. Lindhout, J.P.F., G. Moek, K.E. de Boer and B. van den Berg, "A Method for the Calculation of Three-Dimensional Layers on Practical Wing Configurations," Transactions of ASME, Journal of Fluids Engineering, 103, pp. 104-111 (1981).
41. Head, M.R., "Entrainment in the Turbulent Boundary Layer," A.R.C. R&M No. 3152 (1958).
42. Jischa, M. and K. Homann, "About an Integral Method for Turbulent Boundary Layers Using the Turbulent Energy Equation," Symposium on Turbulent Shear Flows, Pennsylvania State University, pp. 10.43-10.50 (1977).
43. Stock, H.W., "Computation of the Boundary Layer and Separation Lines on Inclined Ellipsoids and of Separated Flows on Infinite Swept Wings," AIAA 13th Fluid and Plasma Dynamics Conference, Snowmass, Colorado (14-16 Jul 1980).
44. Lewkowicz, A.K., D. Hoadley, J.H. Horlock, and H.J. Perkins, "A Family of Integral Methods for Predicting Turbulent Boundary Layers," AIAA Journal, 8, pp. 44-51 (1970).
45. Wheeler, A.J. and J.P. Johnston, "An Assessment of Three-Dimensional Turbulent Boundary Layer Prediction Methods," Transactions of ASME, Journal of Fluids Engineering, 95, pp. 415-421 (1973).
46. Landweber, L., "Characteristics of Ship Boundary Layers," 8th Symposium on Naval Hydrodynamics, Washington, D.C., pp. 449-472 (1970).
47. Landweber, L. and V.C. Patel, "Ship Boundary Layers," Annual Review of Fluid Mechanics, 11, pp. 173-205 (1979).

48. Cumpsty, N.H., "A Critical Examination of the Use of a Two-Dimensional Turbulent Profile Family to Represent Three-Dimensional Boundary Layer," A.R.C. Current Papers 1068, pp. 37 (1970).
49. Hess, J.L., "Review of Integral-Equation Techniques for Solving Potential Flow Problems with Emphasis on the Surface-Source Method," Computer Methods in Applied Mechanics and Engineering, 5, pp. 145-196 (1975).
50. Carmichael, R.L. and L.L. Erickson, "PAN AIR - A Higher Order Panel Method for Predicting Subsonic or Supersonic Linear Potential Flows about Arbitrary Configurations," AIAA 81-1255 (June 1981).
51. Webster, W.C., "The Flow About Arbitrary, Three-Dimensional Smooth Bodies," Journal of Ship Research, 19, pp. 206-218 (1975).
52. East, L.F., "Computation of Three-Dimensional Turbulent Boundary Layers," Aeronautical Research Institute of Sweden (FFA), Technical Note AE-1211 Turbulent Boundary Layers in External Flows: A Report on Euromech 60," Journal of Fluid Mechanics, 71, pp. 815-826 (1975).
53. Humphreys, D.A., "Comparison of Boundary Layer Calculations for a Wing: The May 1978 Stockholm Workshop Test Case," Aeronautical Research Institute of Sweden (FFA), Technical Note AE-1522 (Jan 1979); also, D.A. Humphreys, "Three-Dimensional Wing Boundary Layer Calculated with Eight Different Methods," AIAA Journal, 19, pp. 232-234 (1981).
54. Lindhout, J.P.F., B. van den Berg and A. Elsenaar, "Comparison of Boundary Layer Calculations for the Root Section of a Wing: The September 1979 Amsterdam Workshop Test Case," NLR Report MP-80028 (1980).
55. Larson, L., ed., "SSPA ITTC Workshop on Ship Boundary Layers 1980," Goteborg, Sweden (1981).

56. Kline, S.J., "1980-81 AFOSR-HTTM-Stanford Conference on Complex Turbulent Flows: Comparison of Computation and Experiment," Stanford, CA (1982).
57. Mahgoub, H.E.H. and P. Bradshaw, "Calculation of Turbulent-Inviscid Flow Interactions with Large Normal Pressure Gradients," AIAA Journal, 17, pp. 1025-1029 (1979).
58. Nakayama, A., V.C. Patel and L. Landweber, "Flow Interaction Near the Tail of a Body of Revolution. Part 1: Flow Exterior to Boundary Layer and Wakes; Part 2: Iterative Solution for Flow Within and Exterior to Boundary Layer and Wake," Transactions of ASME, Journal of Fluids Engineering, 98, pp. 531-537; 538-549 (1976).
59. Wang, H. T. and T.T. Huang, "Calculation of Potential Flow Boundary Layer Interaction on Axisymmetric Bodies," International Symposium on Ship Viscous Resistance, pp. 47-57 (1978).
60. Geller, E.W., "Calculation of Flow in the Tail Region of a Body of Revolution," Journal of Hydronautics, 13, pp. 127-129 (1979).
61. Le Balleur, J. C., "Strong Matching Method for Computing Transonic Viscous Flows Including Wakes and Separations. Lifting Airfoils," La Recherche Aerospatiale, 1981-3, pp. 21-45 (1981).
62. Bradshaw, P., "The Analogy Between Streamline Curvature and Buoyancy in Turbulent Shear Flow," Journal of Fluid Mechanics, 36, pp. 177-191 (1969).
63. Bradshaw, P., "Effects of Streamline Curvature on Turbulent Flow," AGARD-AG-169 (1973).
64. Patel, V.C. and Y.T. Lee, "Thick Axisymmetric Boundary Layers and Wakes: Experiment and Theory," International Symposium on Ship Viscous Resistance, SSPA, Goteborg, pp. 4.1-4.20 (1978).

65. Green, J.E., D.J. Weeks and J.W.F. Brooman, "Prediction of Turbulent Boundary Layers and Wakes in Compressible Flow by a Log-Entrainment Method," A.R.C. R&M No. 3791 (1973).
66. East, L.F., "A Representation of Second Order Boundary Layer Effects in the Momentum Integral Equations and in Viscous-Inviscid Interaction," R.A.E. TR-81002 (1981).
67. Cousteix, J. and R. Houdeville, "Singularities in Three-Dimensional Turbulent Boundary-Layer Calculations and Separation Phenomena," AIAA Journal, 19, pp. 976-985 (1981).
68. Cousteix, J., J. Le Balleur, and R. Houdeville, "Calculation of Unsteady Turbulent Boundary Layers in Direct or Inverse Mode, Including Reversed Flows-Analysis of Singularities," La Recherche Aerospatiale 1980-3, pp. 3-13 (1980).
69. East, L.F., P.D. Smith and P.J. Merryman, "Prediction of the Development of Separated Turbulent Boundary Layers by the Log-Entrainment Method," R.A.E. TR-77046 (1977).
70. Whitfield, D.L., T.W. Swafford and J.L. Jacocks, "Calculation of Turbulent Boundary Layers with Separation and Viscous-Inviscid Interaction," AIAA Journal, 19, pp. 1315-1322 (1981).
71. Catherall, D. and K.W. Mangler, "The Integration of the Two-Dimensional Laminar Boundary-Layer Equations Past the Point of Vanishing Skin Friction, Journal of Fluid Mechanics, 26, pp. 163-182 (1966).
72. Carter, J.E., "A New Boundary-Layer Inviscid Interaction Technique for Separated Flow," AIAA Computational Fluid Dynamics Conference, Paper 79-1450, pp. 45-55 (1979).

73. Formery, M. and J. Delery, "Finite Difference Method for the Inverse Model Computation of a Three-Dimensional Turbulent Boundary Layer", La Recherche Aerospatiale 1981-5, pp. 11-21 (1981).
74. Briley, W.R. and H. McDonald, "Computation of Three-Dimensional Horseshoe Vortex Flow Using the Navier-Stokes Equations," 7th International Conference on Numerical Methods in Fluid Dynamics, Stanford University and NASA/Ames (23-27 June 1980).
75. Daiguji, H. and H. Shirahata, "The Secondary Flow About a Circular Cylinder," Bulletin of the JSME, 22, pp. 925-932 (1979).
76. Peake, D.J. and R.D. Galway, "The Three-Dimensional Separation of a Plane Incompressible Laminar Boundary Layer Produced by a Circular Cylinder Mounted Normal to a Flat Plate," National Research Council of Canada Report LR-428 (May 1965).
77. Gessner, F.B., "The Origin of Secondary Flow in Turbulent Flow Along a Corner," Journal of Fluid Mechanics, 58, pp. 1-25 (1973).
78. Gessner, F.B. and A.F. Emery, "A Reynolds Stress Model for Turbulent Corner Flows-Part 1: Development of the Model; Part 2: Comparison between Theory and Experiment," Transactions of ASME, Journal of Fluids Engineering, 98, pp. 261-277 (1976).
79. Arnal, D. and J. Consteix, "Subsonic Flow in a Corner," La Recherche Aerospatiale 1981-1982, pp. 45-62 (1981).
80. McNally, W.D. and P.M. Sockol, "Computational Methods for Internal Flows with Emphasis on turbomachinery," Symposium on Computers in Flow Predictions and Fluid Dynamics Experiments, ASME Winter Annual Meeting, Washington, D.C. (15-20 Nov 1981).

81. Horlock, J.H. and H.J. Perkins, "Annulus Wall Boundary Layers in Turbomachines," AGARD No. 185 (1974).
82. Myring, D.F., "An Integral Prediction Method for Three-Dimensional Turbulent Boundary Layers in Incompressible Flow," R.A.E. TR-70147 (1970).
83. Smith, P.D., "An Integral Prediction Method for Three Dimensional Compressible Turbulent Boundary Layers," A.R.C. R&M No. 3739 (1972).
84. Shanebrook, J.R. and W.J. Sumner, "Crossflow Profiles for Compressible Turbulent Boundary Layers," Journal of Aircraft, 8, pp. 188-189 (1971).
85. Papailiou, K., R. Flot and J. Mathieu, "Secondary Flows in Compressor Bladings," Transactions of ASME, Journal of Engineering for Power, 99, pp. 211-224 (1977k).
86. von Kerczek, C.H., "A New Generalized Cross-Flow Momentum Integral Method for Three Dimensional Ship boundary Layers," Science Applications, Inc. Report SAI-463-82-085-LJ (1982).
87. Patel, V.C. and G. Scheuerer: "Calculation of Two-Dimensional Near and Far Wakes", AIAA Journal 20, pp. 900-907 (1982).
88. Lock, R.C., "A Review of Methods for Predicting Viscous Effects on Aerofoils and Wings at Transonic Speeds," AGARD-CP-291: The Computation of Viscous-Inviscid Interaction, pp. 2.1-2.32 (1980).
89. Lock, R.C. and M.C.P. Firmin, "Survey of Techniques for Estimating Viscous Effects in External Aerodynamics," R.A.E. TR-1900 (1981).
90. Melnik, R.E., "Turbulent Interactions on Airfoils at Transonic Speeds - Recent Development," AGARD-CP-291: The Computation of Viscous-Inviscid Interactions, pp. 10.1-10.34 (1980).
91. Le Balleur, J.C., R. Peyret and H. Viviani, "Numerical Studies in High Reynolds Number Aerodynamics," Computers and Fluids, 8, pp. 1-30 (1980).
92. Green, J.F., "Application of Head's Entrainment Method to the Prediction of Turbulent Boundary Layers and Wakes in Compressible Flow," A.R.C. R&M No. 3788 (1972).

DTNSRDC ISSUES THREE TYPES OF REPORTS

- 1. DTNSRDC REPORTS, A FORMAL SERIES, CONTAIN INFORMATION OF PERMANENT TECHNICAL VALUE. THEY CARRY A CONSECUTIVE NUMERICAL IDENTIFICATION REGARDLESS OF THEIR CLASSIFICATION OR THE ORIGINATING DEPARTMENT.**
- 2. DEPARTMENTAL REPORTS, A SEMIFORMAL SERIES, CONTAIN INFORMATION OF A PRELIMINARY, TEMPORARY, OR PROPRIETARY NATURE OR OF LIMITED INTEREST OR SIGNIFICANCE. THEY CARRY A DEPARTMENTAL ALPHANUMERICAL IDENTIFICATION.**
- 3. TECHNICAL MEMORANDA, AN INFORMAL SERIES, CONTAIN TECHNICAL DOCUMENTATION OF LIMITED USE AND INTEREST. THEY ARE PRIMARILY WORKING PAPERS INTENDED FOR INTERNAL USE. THEY CARRY AN IDENTIFYING NUMBER WHICH INDICATES THEIR TYPE AND THE NUMERICAL CODE OF THE ORIGINATING DEPARTMENT. ANY DISTRIBUTION OUTSIDE DTNSRDC MUST BE APPROVED BY THE HEAD OF THE ORIGINATING DEPARTMENT ON A CASE-BY-CASE BASIS.**